AFOSR-TR- 81-0854

LEVEL II

(12)

AD A109077

DTIC
ELECTE
DEC 30 1981
S D
H

(12) 79

DTIC FILE COPY

Approved for public release;
distribution unlimited.

NEW YORK UNIVERSITY

FACULTY OF ARTS AND SCIENCE

DEPARTMENT OF APPLIED SCIENCE

401164

81 12 29 020

FINAL REPORT

NONLINEAR INSTABILITIES AND LARGE SCALE STRUCTURES IN MIXING LAYERS

R. Vaglio-Laurin and N.S. Liu

NYU/DAS-81-06

SEPTEMBER 1981

This work was supported by the Office of Naval Research under Contract NOOO14-79-C and, in part, by the Office of Scientific Research under Grant AFOSR 80-0184. Submitted to the Journal of Fluid Mechanics for publication October, 1981. (5-259-458;5-259-654).

NEW YORK UNIVERSITY

FACULTY OF ARTS AND SCIENCE

DEPARTMENT OF APPLIED SCIENCE

UNCLASSIFIED
SECURITY CLASSIFICATION OF THIS PAGE (When Data Entered)

REPORT DOCUMENTATION PAGE	READ INSTRUCTIONS BEFORE COMPLETING FORM
1. REPORT NUMBER: AFOSR-TR- 81-0854	2. GOVT ACCESSION NO.: AD-A109077
	3. RECIPIENT'S CATALOG NUMBER
4. TITLE (and Subtitle): NONLINEAR INSTABILITIES AND LARGE SCALE STRUCTURES IN MIXING LAYERS	5. TYPE OF REPORT & PERIOD COVERED: MAY 80 - SEP 80 FINAL
	6. PERFORMING ORG. REPORT NUMBER
7. AUTHOR(s): ROBERTO VAGLIO-LAURIN NAN SUEY LIU	8. CONTRACT OR GRANT NUMBER(s): AFOSR 80-0184
9. PERFORMING ORGANIZATION NAME AND ADDRESS: NEW YORK UNIVERSITY/DEPARTMENT OF APPLIED SCIENCE 26-36 STUYVESANT STREET - BARNEY BLDG NEW YORK, NY 10003	10. PROGRAM ELEMENT, PROJECT, TASK AREA & WORK UNIT NUMBERS: 61102F 2307/A2
11. CONTPOLLING OFFICE NAME AND ADDRESS: AIR FORCE OFFICE OF SCIENTIFIC RESEARCH/NA BOLLING AFB, DC 20332	12. REPORT DATE: SEP 81
	13. NUMBER OF PACES: 74
14. MONITORING AGENCY NAME & ADDRESS(if different from Controlling Office)	15. SECURITY CLASS. (of this report): UNCLASSIFIED
	15a. DECLASSIFICATION/DOWNGRADING SCHEDULE

16. DISTRIBUTION STATEMENT (of this Report)

Approved for public release; distribution unlimited.

17. DISTRIBUTION STATEMENT (of the abstract entered in Block 20, if different from Report)

18. SUPPLEMENTARY NOTES

19. KEY WORDS (Continue on reverse side if necessary and identify by block number)

MIXING LAYER
NONLINEAR UNSTABILITIES
COHERENT STRUCTURES
TRANSITION
TURBULENCE

20. ABSTRACT (Continue on reverse side if necessary and identify by block number)

The dynamics of the large scale structures/vorticity concentrations observed in two-dimensional transitional and turbulent mixing layers are described in terms of a nonlinear inviscid two-dimensional instability model. According to the model the formation and repetitive pairing of the structures reflect a deterministic cyclic mechanism wherein the nonlinear evolution of the finite amplitude instability, which dominates the flow at any one stage, intrinsically provides first excitation of, and then energy transfer to the bound 1/2 sub-harmonic. The key to identifying and modeling the mechanism resides in a

DD FORM 1 JAN 73 1473 EDITION OF 1 NOV 65 IS OBSOLETE

UNCLASSIFIED
SECURITY CLASSIFICATION OF THIS PAGE (When Data Entered)

realistic description of the concurrent changes in the mean flow and in the structure of the wave motion during the amplification, saturation and subsequent modulation of the individual nonlinear instability. Models based on weakly nonlinear stability theory prove inadequate to this task. The cause of failure is identified, and attendant criteria for estimating the applicability of the theory to the present as well as other problems are indicated. By contrast, several salient features of transitional and turbulent mixing layer development are reproduced by the repeated application of a nonlinear model, which describes the life cycle of the individual structure only in terms of the interactive evolution of the mean flow and of the wave motions associated with an appropriate finite amplitude fundamental together with its bound second harmonic. Some views on possible external controls influencing the development of the structures and of the attendant mean flow are inferred on that basis.

NYU/DAS 81-06

TABLE OF CONTENTS

		PAGE NUMBER
ABSTRACT		1
1.	INTRODUCTION	2
2.	FORMULATION OF THE MODELS	7
3.	NUMERICAL PROCEDURES	20
4.	EVOLVING STRUCTURE OF NONLINEAR UNSTABLE WAVE MOTIONS	23
5.	NONLINEAR MECHANISM OF SUBHARMONIC EXCITATION AND AMPLIFICATION	34
6.	DISCUSSION	47
	REFERENCES	58

FIGURES (1 THROUGH 12)

NYU/DAS 81-06

NONLINEAR INSTABILITIES AND LARGE SCALE STRUCTURES IN MIXING LAYERS

R. Vaglio Laurin and N. S. Liu

New York University
Department of Applied Science
New York, New York 10003

ABSTRACT

The dynamics of the large scale structures/vorticity concentrations observed in two-dimensional transitional and turbulent mixing layers are described in terms of a nonlinear inviscid two-dimensional instability model. According to the model, the formation and repetitive pairing of the structures reflect a deterministic cyclic mechanism wherein the nonlinear evolution of the finite-amplitude instability, which dominates the flow at any one stage, intrinsically provides first excitation of, and then energy transfer to, the bound 1/2 subharmonic. The key to identifying and modeling the mechanism resides in a realistic description of the concurrent changes in the mean flow and in the structure of the wave motion during the amplification, saturation and subsequent modulation of the individual nonlinear instability. Models based on weakly nonlinear stability theory prove inadequate to this task. The cause of the failure is identified, and attendant criteria for estimating the applicability of the theory to the present as well as other problems are indicated. By contrast, several salient features of transitional and turbulent mixing layer development are

reproduced by the repeated application of a nonlinear model, which describes the life cycle of the individual structure only in terms of the interactive evolution of the mean flow and of the wave motions associated with an appropriate finite amplitude fundamental together with its bound second harmonic. Some views on possible external controls influencing the development of the structures and of the attendant mean flow are inferred on that basis.

1. INTRODUCTION

Recent experiments by Wygnanski et al (1979a) and by Browand and Troutt (1980) clearly demonstrate that the quasi two dimensional large scale coherent structures/vorticity concentrations first observed by Brown and Roshko (1974) persist in turbulent mixing layers. The structures, with principal alignment in the spanwise direction, rapidly approach an asymptotic state where their mean transversal dimensions as well as spanwise correlation length become functions only of the local mixing layer thickness δ_ω. Their mean distance of travel between pairings then depends only on the ratio $(\delta_\omega/\lambda) = \delta_\omega(U_1 + U_2)/(U_1 - U_2)$--where U_1 and U_2 denote the velocities of the two streams partaking in the mixing--so that, for a fixed velocity ratio λ, the length of the pairing process also scales with the local thickness δ_ω. Thus, the repetitive occurrence of a deterministic self-preserving mechanism of intrinsic subharmonic generation is strongly suggested. The view is supported by the observation that initially forced mixing layers (Wygnanski et al 1979b, Ho and Huang 1980) exhibit a rapid return to the behavior of unforced layers following the initial formation of a single large structure by the simultaneous agglomeration of several smaller ones.

Whereas the pairing of structures/vortices is largely responsible for the turbulent mixing layer growth (Winant and Browand 1974, Roshko 1976), a

quantitative understanding of the attendant dynamics is of distinct interest from the dual viewpoint of developing flow models based on first principles and of establishing a rational basis for possible flow control concepts. Available models of the pairing process rely on numerical analyses of the unsteady twodimensional flows which evolve either from an initial parallel "base shear flow" perturbed by one or more excited eigenmodes of arbitrarily prescribed small amplitude and relative phase (e.g. Zabusky and Deem 1971, Patnaik et al 1976), or from an assembly of discrete line vortices initially arranged in cyclic arrays with arbitrarily prescribed small lateral displacements and/or offsets (e.g., Acton 1976), Aref and Siggia 1980) . In either case solutions are obtained subject to boundary conditions which assume periodicity of all flow variables in the streamwise direction over the length of the computational domain. Many detailed features experimentally observed during the nonlinear phases of transition in selected free shear flows have successfully been reproduced by these models in conjunction with initial conditions which realistically reflect those encountered in the experiments. However, the comparisons have typically been restricted to limited intervals of space in the experiments and corresponding time in the theoretical predictions. With few exceptions, e.g., the calculation reported by Aref and Siggia (1980), the onset of a cyclic self-preserving process of 1/2 subharmonic generation and amplification, such as indicated by the observations of coherent structures in mixing layers, has not been demonstrated analytically. Since the numerical solutions are deterministic and uniquely defined by the assumed initial conditions and the non controversial boundary conditions, it is difficult to understand how they could predict self-preserving vortex pairing over distances which scale with the local layer

thickness δ_ω in unforced mixing layers, and rapidly recover the same self-preserving process in forced mixing layers, which evolve from obviously different initial conditions. Thus, the issue of understanding the dynamics of the scale change undergone by the structures as they convect downstream is not fully settled.

The observed rapid recovery of self-preserving vortex pairing over lengths which scale with the local mixing layer thickness, independently of the initial and external disturbance spectrum, suggests that the operative mechanism may be one where 1) the excitation of the 1/2 subharmonic is intrinsic to the nonlinear evolution of the finite amplitude instabilities which control the formation of the individual structures, and 2) the subsequent amplification of the subharmonic drains energy from the preexisting instability so that memory of the specific initial conditions is largely lost after one or a few structure life cycles. This is the proposition elaborated in this paper. Its demonstration clearly depends on a realistic description of the history and structure of nonlinear wave motions associated with individual finite amplitude instabilities and on a study of self-induced modulations which result in interacting pairs of such instabilities having frequency ratios of about 2. The paper devotes much attention to the analysis of these specific problems.

In order to avoid the large labor and cost entailed by simulations of spatially developing flows, where the streamwise extent of the computational domain must encompass several vortex pairing lengths, our investigations address the problem of temporally developing mixing layers, where a computational domain with streamwise extent restricted to two eddy sizes allows analysis of the vortex pairing process and assessment of its self preserving nature. In doing so we recognize that the time evolution of the unsteady shear layer,

statistically homogeneous in the streamwise direction, and the space evolution of the laboratory mixing layer, statistically stationary in time, are not strictly equivalent,since one flow cannot be reduced to the other by a Galilean transformation. Accordingly, we employ due caution in transposing results from one situation to the other, especially for what concerns the interactions among instability pairs, which are known to be dispersive in the spatial amplification case (Michalke 1965) but non-dispersive in the temporal amplification case (Michalke 1964). The relevance of this caveat to the study of vortex pairing is evidenced by Petersen's (1978) experimental finding that"... the first pairing occurred where the mixing layer became sufficiently thick, owing to nonlinearities and entrainment, that a subharmonic wave had a phase velocity that matched the convection speed of the vortex ring."

Our inquiries into the structure of the wave motion associated with instabilities of small but finite amplitude, growing at a finite rate, largely address the central tenet of weakly nonlinear theories, viz., that the eigenfunctions given by linear theory continue to yield an adequate representation of the motion in the nonlinear case. Since experiments (e.g., Miksad 1972) clearly show that significant variations of mean flow and maximum shear accompany the growth of instabilities even at modest amplitudes, we relinquish the classical assumption of invariant eigenfunction shape (Stuart 1960) in favor of the Meksyn and Stuart approach (1951), which we rederive in the context of multiple scales methods (e.g., Nayfeh 1973) together with a self-consistent equation for the time rate of change of the disturbance energy. We then assess the predictions of the extended Meksyn and Stuart model by comparing them with Miksad's (1972) hot wire measurements in the nonlinear stages of free shear layer transition as well as with the predictions of a nonlinear model largely patterned after those of Zabusky and Deem (1971) and Patnaik et al (1976). Unfortunately,

the assessment proves negative, so that all our subsequent considerations necessarily rely on the nonlinear model. On the positive side, the reason for the failure of the Meksyn and Stuart approach is identified, and attendant criteria for estimating the applicability of that model in other nonlinear instability problems are indicated.

Our inquiries into the mechanism of subharmonic generation and amplification largely stem from the predictions of the nonlinear model for the concurrent evolutions of the mean flow and of the wave motion associated with a finite amplitude instability undergoing saturation and subsequent self-induced modulation of both amplitude and structure. Whereas the frequency of the modulation is close to that of the subharmonic, and the phase velocity of the subharmonic compatible with the prevailing mean flow structure matches the convection speed of the vorticity concentrations generated by the saturated instability, we find here conditions intrinsically conducive to the initiation of vortex pairing. A calculation employing the nonlinear model to describe the development of the unsteady shear layer which evolves from such initial conditions (including the attendant initial structures of the fundamental and subharmonic wave motions) allows us then to follow the pairing process to subharmonic saturation, and to demonstrate the cyclic nature of that process by the favorable comparison of the mean flow and wave motion prevailing at the beginning and at the end of the cycle.

In the main body of the paper, the elaboration of our inquiries, and the presentation of the attendant results, are prefaced by a derivation of the relevant analytical models in the context of selected experimental data, which provide guidelines for that derivation (Section 2), as well as benchmarks for the

subsequent assessments (Sections 4 and 5). Numerical procedures used in the implementation of the models are presented in Section 3.

2. FORMULATION OF THE MODELS

Based on the experimental observation (Roshko 1976) that the large organized structures of mixing layers are not affected by the small scale turbulence appearing at the higher Reynolds numbers, we take the threefold view that: 1) essentially the same cyclic nonlinear mechanism governs the formation and the pairing of structures throughout the nonlinear transitional and turbulent regimes; 2) in each cycle the mechanism is only associated with a few discrete large scale dominant inviscid twodimensional instabilities, whose energy first grows and then decays along the lines indicated by measurements in transitional flows; 3) the high Reynolds number small scale turbulence, bound to the large scale structures and generated by a hierarchy of secondary instabilities intrinsic to the flow patterns associated therewith, plays a negligible role in the dynamics of the individual cycle, and merely provides the conduit for cascading the residual energy of large scale instabilities dominant in previous cycles. In support of these views we submit that the predominance of a two-dimensional mechanism is not precluded by the experimental finding (Browand and Troutt 1980) that the structures are not strictly spanwise and two-dimensional but, instead, may be skewed and branched. The observed ratio between the spanwise correlation length of the structures and the local mixing layer thickness δ_ω approaches a lower bound of about 3 for 20% correlation coefficient in flows characterized by a velocity ratio $\lambda \simeq 1$ and by a sufficiently high Reynolds number $(U_1-U_2)\delta_\omega/\nu$. In these flows the streamwise separation between structures, as well as their travel distance between pairings,

are of the order of 3 to $4\delta_\omega$; thus, the wavelength characteristic of the observed spanwise skewness is distinctly larger than the lengths characteristic of the streamwise instabilities controlling the evolution of the structures.* Under those conditions only a linear, zero average, spanwise modulation of the instabilities and their nonlinear dynamics should accompany, and manifest itself in, the skewness; accordingly, consideration of the nonlinear processes in a spanwise-averaged twodimensional approximation is indicated. In that connection we also remark that a secondary Taylor-type instability--intrinsic to, and bound with, the flow pattern relative to the evolving vorticity concentrations/vorticity braids characteristic of the structures--is presumably responsible for the observed skewness. Pending a quantitative analysis of this instability and its interactions with the streamwise instabilities, we note that the experimentally observed invariant scaling of the spanwise correlation length with the layer thickness δ_ω indicates synchronous cycles of period doubling and attendant energy transfer in wavenumber space for the dominant streamwise and spanwise instabilities. Since period doubling implies at least a half revolution of fluid elements within the developing subharmonic cat's eye, and since spanwise and streamwise r.m.s.. velocities are at best comparable, the shorter wavelength streamwise instabilities necessarily control the process; the spanwise instabilities, paced by the stage of development of the supporting large scale structures in streamwise planes, then follow, and just respond to, that development. Thus, the study of large scale structure dynamics in a two-dimensional approximation is indicated again. In this approximation we then approach the specific problems posed in the introduction.

*The measurements of Wygnanski et al (1979a) indicate much larger spanwise correlation lengths for a velocity ratio $\lambda = 0.4$.

In order to assess what constitutes a realistic description of the history and structure of nonlinear wave motions associated with individual finite amplitude instabilities we consider the nonlinear time development of homogeneous inviscid incompressible two dimensional unstable shear flows. With reference to cartesian coordinates (x, y), we assume that the initial state of motion results from the superposition of a single, small amplitude, excited eigenmode, periodic in x and t (with wavenumber α and frequency β) upon a mean (x-averaged) parallel velocity field; that is, at $t = 0$

$$\underline{V}(x, y, 0) = [U(y,0) + u(x, y, 0), v(x,y,0)] \tag{1}$$

We describe the time evolution of the flow in terms of the stream function $\tilde{\psi}(x,y,t)$ which must satisfy the vorticity conservation equation

$$(\nabla^2\tilde{\psi})_t + \tilde{\psi}_y(\nabla^2\tilde{\psi})_x - \tilde{\psi}_x(\nabla^2\tilde{\psi})_y = 0 \tag{2}$$

subject to the initial conditions (1) and to the boundary conditions

$$y \to \pm\infty \qquad \tilde{\psi}_x \to 0 \tag{3-a}$$

if the flow is unbounded, or the boundary conditions

$$y = \pm y_w \qquad \tilde{\psi}_x = 0 \tag{3-b}$$

if the flow is bounded by rigid walls at $y = \pm y_w$.

We seek solutions of equation (2) under the assumption that, for all times $t > 0$, the stream function $\tilde{\psi}$ may be resolved into a mean flow contribution $\Psi(y,t)$ and a disturbance contribution $\varepsilon\psi(x,y,t)$, the latter possessing small but finite amplitude characterized by the parameter $\varepsilon << 1$, as well as x-periodicity with wavelength $(2\pi/\alpha)$; thus

$$\tilde{\psi}(x,y,t) = \Psi(y,t), + \varepsilon\psi(x,y,t) \tag{4}$$

Substitution of (4) into (2) yields

$$(\nabla^2\Psi + \varepsilon\nabla^2\psi)_t + \varepsilon\,[\Psi_y\,(\nabla^2\psi)_x - \psi_x\,(\nabla^2\Psi)_y]$$

$$+\,\varepsilon^2[\psi_y(\nabla^2\psi)_x - \psi_x\,(\nabla^2\psi)_y] = 0 \tag{5}$$

and upon x-averaging

$$(\nabla^2\Psi)_t + \varepsilon^2\langle\psi_y(\nabla^2\psi)_x - \psi_x(\nabla^2\psi)_y\rangle = 0 \tag{6}$$

which is the equation governing the time evolution of the mean flow. The equation describing the evolution of the periodic disturbance follows readily upon subtraction of (6) from (5), viz.

$$(\nabla^2\psi)_t + \Psi_y(\nabla^2\psi)_x - \psi_x(\nabla^2\Psi)_y$$

$$+\varepsilon[\psi_y(\nabla^2\psi)_x - \psi_x(\nabla^2\psi)_y - \langle\psi_y(\nabla^2\psi)_x - \psi_x(\nabla^2\psi)_y\rangle] = 0 \tag{7}$$

Equation (6) indicates that, if the disturbance stream function remains of order unity under differentiation with respect to the space coordinates, the mean flow vorticity $(\nabla^2\Psi)$ varies on a slow time scale $\tau = \varepsilon^2 t$. Under these conditions the solution of (7) may be sought by the method of multiple scales (e.g., Nayfeh 1973), and a uniform expansion for the disturbance stream function in powers of ε may be obtained according to

$$\varepsilon\psi(x,y,t) = \sum_{n=1}^{3} \varepsilon^n \psi_n(x,y,t,\tau) \tag{8}$$

If, in line with our assumption, a single eigenmode is excited at $t = 0$, the leading term of the solution (8) must have the form

$$\psi_1(x,y,t,\tau) = 1/2[A_1(\tau)\,\zeta_1(y,\tau)\,e^{i\theta} + \text{c.c.}] \tag{9}$$

where $\dfrac{\partial\theta}{\partial x} = \alpha \qquad \dfrac{\partial\theta}{\partial t} = -\beta(\tau)$

Substitution into (7) then shows that the function $\zeta_1(y,\tau)$ must satisfy the Rayleigh equation

$$L_1(\zeta_1) = (U\alpha - \beta)(\zeta_{1yy} - \alpha^2\zeta_1) - \alpha U_{yy}\zeta_1 = 0 \tag{10}$$

with the homogeneous boundary conditions

$$y \to \pm\infty \qquad \zeta_1 \to 0 \tag{11}$$

but that the function $A_1(\tau)$ remains undetermined at this level of approximation. The equation governing the presumed slow time evolution of the mean flow to this leading order is obtained readily from (6) and (9), viz

$$U_\tau = -1/2\ \alpha|A_1|^2 \exp\left(2\int_0^t \beta_i\, dt\right)\ \mathrm{Im}(\zeta_1\zeta^*_{1yy}) \tag{12-a}$$

where ζ_1^* denotes the complex conjugate of ζ_1 and $\beta_i = \mathrm{Im}(\beta)$. If (10) is used to express ζ^*_{1yy} in terms of U and ζ_1^*, (12-a) may be recast in the form

$$U_\tau = \frac{\alpha^2}{2}|A_1|^2 \exp\left(2\int_0^t \beta_i dt\right)\beta_i\ |U\alpha - \beta|^{-2}|\zeta_1|^2 U_{yy} \tag{12-b}$$

which clearly is of parabolic type, with space and time dependent effective diffusivity, as long as $\beta_i > 0$. Successive differentiations of (12-a,b) with respect to y readily yield expressions for the slow time variations of the slope and curvature of the mean velocity profile $U(y,\tau)$, viz.

$$U_{y\tau} = -\frac{1}{2}\alpha|A_1|^2 \exp\left(2\int_0^t \beta_i dt\right)\mathrm{Im}(\zeta_1\zeta^*_{1yy})_y =$$

$$-\frac{\alpha^2}{2}|A_1|^2\exp\left(2\int_0^t \beta_i dt\right)\beta_i\ |U\alpha - \beta|^{-2}\ (U_{yy}|\zeta_1|_y^2 + U_{yyy}|\zeta_1|^2) -$$

$$2\alpha^2|U\alpha - \beta|^{-2}\ U\,U_y\,U_\tau \tag{13}$$

$$U_{yy\tau} = -\frac{1}{2}\alpha|A_1|^2 \exp\left(2\int_0^t \beta_i\, dt\right) \mathrm{Im}\,(\zeta_1\zeta_{1yy}^*)_{yy} =$$

$$\frac{\alpha^2}{2}\ |A_1|^2 \exp\left(2\int_0^t \beta_i\, dt\right) \beta_i\ |U\alpha - \beta|^{-2} \times$$

$$(U_{yy}|\zeta_1|^2{}_{yy} + 2\,U_{yyy}\,|\zeta_1|_y^2 + U_{yyyy}\,|\zeta_1|^2) \qquad (14)$$

$$-2\alpha^2\ |U\alpha - \beta|^{-2}\ [(UU_y)_y\ U_\tau + 2\,U\,U_y U_{y\tau}]$$

Clearly equation (10) and (12) merely reproduce the model of Meksyn and Stuart (1951) for the study of finite disturbances. The derivation by the multiple scales method clarifies the crucial underlying assumption of slow variation of the mean flow as well as provides the framework for a systematic evaluation of the function $A_1(\tau)$ (see below) without appeal to the heuristic energy considerations adopted in the original model. The equations (13) and (14) have no direct role in the determination of the flow according to the model. They are presented here because experience with solutions of the Rayleigh equation (10) indicates that the eigenfunction ζ_1 and the associated eigenvalue β are quite sensitive to the curvature U_{yy} of the mean velocity profile. An examination of (14) then provides the key to the a posteriori assessment of the conditions where slow time variation of the mean flow and attendant description of the disturbance evolution according to the multiple scales method, may realistically be assumed. Toward that objective, we need to determine the equations governing the second order $o(\varepsilon^2)$ and third order $o(\varepsilon^3)$ contributions to the solution (8); this is done below.

Elaboration of (7) in the context of the solution (8) shows that the contribution ψ_2 to the disturbance stream function must have the form

$$\psi_2(x,y,t,\tau) = \frac{1}{4}\,[A_1^2(\tau)\,\zeta_2(y,\tau)\,e^{2i\theta} + c.c.] \tag{15}$$

the function ζ_2 being the solution of the equation

$$L_2(\zeta_2) = (U\alpha - \beta)\,(\zeta_{2yy} - 4\alpha^2\,\zeta_2) - \alpha U_{yy}\,\zeta_2 =$$

$$\frac{\alpha}{2}\,(\,\zeta_1\,\zeta_{1yyy} - \zeta_{1y}\,\zeta_{1yy}) \tag{16}$$

subject to the boundary conditions

$$y \to \pm\,\infty \qquad \zeta_2 \to 0 \tag{17}$$

However, the function $A_1(\tau)$ still remains undetermined. As usual in weakly nonlinear stability theories, an equation for $A_1(\tau)$ is obtained upon consideration of the contribution $o(\varepsilon^3)$ to the solution (8). Elaboration of (7) to $o(\varepsilon^3)$ shows that the inhomogeneous part of the equation for ψ_3 includes, among others, terms proportional to $\exp(i\theta)$, which are contributed by the derivative of ψ_1 with respect to the slow time variable τ. Secular terms in the particular solution for ψ_3, and the attendant nonuniformity of the expansion (8), can then be avoided only by seeking the particular solution in the form

$$\psi_3(x,y,t,\tau) = \frac{1}{2}\,[\,A_1(\tau)\,|A_1(\tau)|^2\zeta_3(y,\tau)\,e^{i\theta} + c.c.] \tag{18}$$

the function ζ_3 being the solution of the equation

$$L_1(\zeta_3) = (U\alpha - \beta)\,(\zeta_{3yy} - \alpha^2\zeta_3) - \alpha U_{yy}\zeta_3 =$$

$$i(A_1\,|A_1|^2)^{-1}(A_1 g_1)_\tau + \exp[i(\theta - \theta^*)]\,g_2 \tag{19}$$

where

$$g_1(y,\tau) = (\zeta_{1yy} - \alpha^2\zeta_1) \tag{20-a}$$

$$g_2(y,\tau) = [\alpha(2\zeta_2\zeta^*_{1yyy} + \zeta_{2y}\,\zeta^*_{1yy}) - 2\alpha\,\zeta^*_{1y}\,(\zeta_{2yy} - 3\alpha^2\zeta_2) -$$
$$\alpha\zeta^*_1(\zeta_{2yy} - 3\alpha^2\zeta_2)_y]/4 \tag{20-b}$$

subject to the boundary conditions

$$y \to \pm \infty \qquad \zeta_3 \to 0 \tag{21}$$

Clearly integrability of (19) requires that

$$\int_{-\infty}^{\infty} \{A_{1\tau} g_1 + A_1 g_{1\tau} - i A_1 |A_1|^2 \exp [i(\theta - \theta^*)] g_2\} \tilde{\zeta}_1 \, dy = 0$$

where $\tilde{\zeta}_1(y,\tau)$ denotes the solution of the equation adjoint to the Rayleigh equation, viz

$$(U\alpha - \beta)(\tilde{\zeta}_{1yy} - \alpha^2 \tilde{\zeta}_1) + 2\alpha U_y \tilde{\zeta}_{1y} = 0 \tag{22}$$

Accordingly $A_1(\tau)$ must satisfy the ordinary differential equation

$$h_1 A_1' + h_2 A_1 + h_3 A_1 |A_1|^2 = 0 \tag{23}$$

where

$$h_1(\tau) = \int_{-\infty}^{\infty} g_1(y,\tau) \, \tilde{\zeta}_1(y,\tau) \, dy \tag{24-a}$$

$$h_2(\tau) = \int_{-\infty}^{\infty} [(\partial/\partial\tau) g_1(y,\tau)] \, \tilde{\zeta}_1(y,\tau) \, dy \tag{24-b}$$

$$h_3(\tau) = -i \exp [i(\theta - \theta^*)] \int_{-\infty}^{\infty} g_2(y,\tau) \, \tilde{\zeta}_1(y,\tau) dy \tag{24-c}$$

Equation (23) embodies the extension of the Meksyn and Stuart model yielded by multiple scales considerations. Interestingly enough, if the τ dependence of the eigenfunction is ignored, i.e., if $g_{1\tau} = h_2 = 0$ in (24-b), equation (23) reduces to the classical result of Stuart (1960); thus both the Meksyn and Stuart and the Stuart models arise as particular cases in the present context.

The derivative $g_{1\tau}$ in (24-b) and the coefficient h_2 in (23) are retained here; they are evaluated by noting that, since the eigenfunction ζ_1 satisfies the Rayleigh equation (10), the derivative $\zeta_{1\tau}$ must satisfy the equation

$$L_1(\zeta_{1\tau}) = (U\alpha - \beta)(\zeta_{1\tau yy} - \alpha^2 \zeta_{1\tau}) - \alpha U_{yy} \zeta_{1\tau} = (\beta_\tau - \alpha U_\tau)(\zeta_{1yy} - \alpha^2 \zeta_1) + \alpha U_{yy\tau} \zeta_1 \tag{25}$$

readily derivable from (10) upon differentiation with respect to the slow time τ.

Equation (25) is also subject to an integrability condition which yields an ordinary differential equation for the τ dependent eigenvalue $\beta(\tau)$, namely

$$\beta' = [h_4(\tau)/h_1(\tau)] \quad \text{or} \quad \beta(\tau) - \beta(0) = \int_0^\tau (h_4/h_1)\, d\tau \tag{26}$$

where

$$h_4(\tau) = -\alpha \int_{-\infty}^{\infty} U_\tau (\zeta_1 \tilde{\zeta}_{1yy} + 2\zeta_{1y}\tilde{\zeta}_{1y} + \alpha^2 \zeta_1 \tilde{\zeta}_1)\, dy \tag{27}$$

With this condition, which merely reflects the association between the τ-dependent eigenvalues β and eigensolutions ζ_1 of equation (10), the formulation of the extended Meksyn and Stuart model is completed. Its application to determine the evolution of an inviscidly unstable free shear flow subject to finite amplitude instabilities involves a stepwise advancement of the solution in time. Given the initial mean velocity field $U(y, 0)$ and the wavenumber α as well as the initial amplitude $A_1(0)$ of the disturbance, the unit step in that process, between times 0 and $\Delta\tau$, involves sequentially: i) the integration of equations (10), (22) and (16) to determine, respectively, the eigenvalue $\beta(0)$ together with the function $\zeta_1(y,0)$ and the functions $\tilde{\zeta}_1(y,0)$, $\zeta_2(y,0)$; ii) the evaluation of $U_\tau(y,0)$, and $U_{yy\tau}(y\ 0)$, $\beta'(0)$ from (12), (14) and (26), respectively, and the consequent determination of $\zeta_{1\tau}(y,0)$ by integration of (25); iii) the integration of (23) and (12-b) to obtain $A_1(\Delta\tau)$ and $U(y,\Delta\tau)$, whereupon the next step can be started. Numerical procedures for these calculations are presented in Section 3, and an assessment of the attendant predictions for the evolving structure of the wave motion associated with a finite amplitude instability is set forth in Section 4.

Whereas measurements, even if detailed and spectrally resolved, do not usually provide much information about those features of nonlinear instability waves -- viz., transversal variation in phase and associated velocity as well as vorticity fields -- which are most important for the realistic evaluation and refinement of a theoretical model, the assessment of Section IV includes a three way comparison among available experimental data, predictions of the (weakly nonlinear) extended Meksyn and Stuart model, and predictions of a strongly nonlinear model. The choice of the nonlinear model is tailored to both lines of inquiry reported in the paper, namely: the identification of the cyclic subharmonic generation mechanism in mixing layers and the description of the detailed structure of the nonlinear wave motions associated therewith.* As stated above, we seek to demonstrate that the dynamics of two-dimensional inviscidly unstable transitional and turbulent shear flows are dominated by the same deterministic, self-preserving, repetitive process of subharmonic generation wherein the nonlinear evolution of an individual finite-amplitude, two dimensional, streamwise-propagating instability intrinsically provides mean flow growth as well as cyclic excitation of, and subsequent energy transfer to, its own 1/2 subharmonic. In this view a restricted class of nonlinear instability processes is singled out as governing the development of turbulent mixing layers. Specifically, the initial formation of vorticity concentrations in the transition region is associated with the self-limiting nonlinear growth of a single dominant inviscid instability -- the fundamental -- whose selection is governed by a convolution of the disturbance environment with the receptivity (Tam 1978) and the frequency/

* The failure of the weakly nonlinear model in describing the structure of individual instabilities (see Section 4) preempts its extension to the subharmonic generation problem.

amplification rate properties (Michalke 1964) of the initial mixing layer. The evolution of the fundamental is strongly influenced by the concurrent distortion of the mean flow, but is largely unaffected by the concurrent excitation of harmonics (Zabusky and Deem 1971). Upon saturation the fundamental undergoes a self-induced modulation (the vortex nutation observed by Zabusky and Deem 1971, Patnaik et al 1976, Miura and Sato 1978), which affects the amplitude and the structure of the wave motion, as well as the distortion of the mean flow. As we shall demonstrate in section 5, the frequency of this modulation is nearly 1/2 that of the saturated fundamental, while the concurrent mean flow distortion is such that the subharmonic frequency closely approaches those of the maximum amplification rate spatial and temporal instabilities for the prevailing mean flow. Since the phase velocities of these instabilities and of the fundamental are then essentially the same, 1/2 subharmonic excitation, with well defined initial amplitude as well as structure of the attendant wave motion, ensues from the modulation of the fundamental. The intrinsically excited subharmonic then amplifies, draining energy from the fundamental as well as from further distortion of the mean flow. However, its growth is again self-limiting and such that, at saturation, the original fundamental becomes nearly spent, while the structures of the mean flow and of the subharmonic wave motion reproduce, except for a doubling of all length scales, the structures that prevailed at the earlier time of fundamental saturation. A self-preserving process of cyclic nonlinear subharmonic generation and mean flow development follows necessarily.

Whereas only two waves (a fundamental and its second harmonic interacting with each other as well as with the mean flow) are active at any stage of the nonlinear wave cycle postulated above, our nonlinear model seeks solutions of the

equations (6) and (7) under the assumption that the perturbation stream function ψ may be described at all times by a Fourier series in x truncated at the second term, viz

$$\psi(x,y,t) = 1/2[\sum_{n=1}^{2} \phi_n (y,t)e^{in\alpha x} + c.c.] \quad (28)$$

With this assumption the modal structure of the evolving flow is clearly manifested at all times, and the complexity as well as cost of the numerical integrations are considerably reduced. In its support we note that the numerical results of Miura and Sato (1978), who adopted the Fourier series approximation, and those of Zabusky and Deem (1971), who directly integrated the time-dependent incompressible Navier-Stokes equations, exhibit qualitatively identical saturation and post-saturation behaviors for finite amplitude instabilities in free shear flows. Thus, the departure of finite amplitude instabilities from an initially sinusoidal spatial shape (Patnaik et al 1976) seemingly plays a secondary role in their development. However, further scrutiny may be in order as to the influence of that departure on the onset and evolution of small scale secondary instabilities -- e.g., those responsible for the skewness and apparent branching of the mixing layer structures -- which are sensitive to the details of the flow pattern relative to those very structures.

Substitution of the assumed form of solution (28) into (6) and (7) readily yields the system of coupled nonlinear partial differential equations which govern the concurrent time evolution of the mean flow and the selected two dimensional disturbance modes, namely

$$U_t = \varepsilon^2 \frac{i\alpha}{4}[\phi_1\phi^*_{1yy} - \phi^*_1\phi_{1yy} + 2(\phi_2\phi^*_{2yy} - \phi^*_2\phi_{2yy})] \quad (29\text{-a})$$

$$[i(\partial/\partial t) - U\alpha](\phi_{1yy} - \alpha^2\phi_1) + \alpha U_{yy}\,\phi_1 =$$

$$-\varepsilon\frac{\alpha}{2}[2\phi_2(\phi^*_{1yy} - \alpha^2\phi^*_1)_y - \phi^*_1(\phi_{2yy} - 4\alpha^2\phi_2)_y + \qquad (29\text{-b})$$

$$\phi_{2y}(\phi^*_{1yy} - \alpha^2\phi^*_1) - 2\phi^*_{1y}(\phi_{2yy} - 4\alpha^2\phi_2)]$$

$$[i(\partial/\partial t) - 2U\alpha](\phi_{2yy} - 4\alpha^2\phi_2) + 2\alpha U_{yy}\,\phi_2 =$$

$$-\varepsilon\frac{\alpha}{2}[\phi_1(\phi_{1yy} - \alpha^2\phi_1)_y - \phi_{1y}(\phi_{1yy} - \alpha^2\phi_1)] \qquad (29\text{-c})$$

to be integrated numerically subject to prescribed initial conditions $U(y,0)$, $\phi_1(y,0)$, $\phi_2(y,0)$ and to the boundary conditions

$$y \to \pm\infty \qquad U(y,t) \to U(y,0)$$
$$\phi_1(y,t) \to 0 \qquad \phi_2(y,t) \to 0 \qquad (30)$$

Procedures for this numerical integration are presented in the following section, and attendant results, relevant to our inquiries, are reported and discussed in Sections 4 and 5.

3. NUMERICAL PROCEDURES

As pointed out in Section 2, the unit problem of determining the evolution of the motion associated with a nonlinear instability over a time interval $\Delta\tau$ according to the extended Meksyn and Stuart model involves the sequential integration of equations (10), (22), (16), (25), (23) and (12-b). The integration of equation (10) to determine $\zeta_1(y,\tau)$ poses a classical eigenvalue problem, which is solved by iteration. Given a trial eigenvalue $\beta(\tau)$, two linearly independent solutions $\zeta_1^{(1)}$ and $\zeta_1^{(2)}$, satisfying the asymptotic behavior $\zeta_1^{(i)} \to C_1^{(i)}(\tau) \exp(-\alpha y)$ for $y \to \infty$, are determined by numerical integration using a variable order Adams predictor-corrector method to march from large y toward y = 0, where the condition $[\mathrm{Re}(\zeta_{1y}^{(1)})/\mathrm{Re}(\zeta_{1y}^{(2)})] = [\mathrm{Im}(\zeta_1^{(1)})/\mathrm{Im}(\zeta_1^{(2)})]$ is to be satisfied. The value of β is incremented using a Newton-Raphson scheme, and the numerical integrations are repeated, until the condition on y = 0 is satisfied. The final solutions $\zeta_1^{(i)}$ are linearly combined so that $\mathrm{Re}\,[\zeta_{1y}(0,\tau)] = \mathrm{Im}\,[\zeta_1(0,\tau)] = 0$, and then normalized so that $\mathrm{Re}\,[\zeta_1(0,\tau)] = 1$. Exactly the same procedure is then followed to determine $\tilde{\zeta}_1(y,\tau)$ by numerical integration of (22); however, no iteration in β is required because (22) is adjoint to (10). The determination of $\zeta_2(y,\tau)$ by integration of the nonhomogeneous equation (16) subject to the homogeneous boundary conditions (17) is unique, and reducible to the evaluation of the particular integral, because no complementary functions of (16) exist which satisfy (17). Two particular integrals $\zeta_2^{(1)}$ and $\zeta_2^{(2)}$, satisfying the asymptotic behavior $\zeta_2^{(i)} \to C_2^{(i)} \exp(-2\alpha y)$ for $y \to \infty$, are first determined by numerical integration using the aforenoted Adams method to march from large y to y = 0; the final solution is then obtained by the linear combination $\zeta_2 = D_2\zeta_2^{(1)} + (1 - D_2)\,\zeta_2^{(2)}$, which satisfies the conditions $\mathrm{Re}[\zeta_{2y}(0,\tau)] = \mathrm{Im}[\zeta_2(0,\tau)] = 0$

provided

$$D_2 = -\Delta^{-1}[(\zeta_2^{(1)*} - \zeta_2^{(2)*})\ \mathrm{Re}(\zeta_{2y}^{(2)}) + i\ (\zeta_{2y}^{(1)*} - \zeta_{2y}^{(2)*})\ \mathrm{Im}\ (\zeta_2^{(2)})]_{y=0}$$

with

$$\Delta = \mathrm{Re}[(\zeta_2^{(1)} - \zeta_2^{(2)})\ (\zeta_{2y}^{(1)*} - \zeta_{2y}^{(2)*})]_{y=0}$$

The integration of (25), subject to the boundary conditions $\zeta_{1\tau} \to 0$ for $y \to \infty$ and $\zeta_{1\tau} = 0$ for $y = 0$, is reduced to the evaluation of quadratures by the substitution

$$\zeta_{1\tau}(y,\tau) = \zeta_1(y,\tau) \int_0^y \eta_1(y,\tau)\, dy$$

which transforms (25) into the equation

$$\eta_{1y} + 2\zeta_1^{-1}\zeta_{1y}\ \eta_1 = f(y,\tau)$$

with

$$f(y,\tau) = (U\alpha - \beta)^{-1}\ [\alpha U_{yy\tau}\zeta_1 - (U_\tau\ \alpha - \beta')\ (\zeta_{1yy} - \alpha^2\zeta_1)]$$

The solution is

$$\eta_1(y,\tau) = \zeta_1^{-2} \int_\infty^y \zeta_1\, f\, dy$$

Upon this determination of $\zeta_{1\tau}(y,\tau)$ the amplitude function $A_1(\tau + \Delta\tau)$ is calculated from (23) and, finally, the mean velocity $U(y,\tau + \Delta\tau)$ is obtained by numerical solution of the nonlinear parabolic equation (12-b). In that connection a standard, stable, implicit, second order accurate scheme, where time and space derivatives are approximated by centered differences, is used to convert (12-b) into a system of simultaneous linear equations for the unknowns $w_j^{n+1} = (U_j^{n+1} - U_j^n) = [U_j(\tau + \Delta\tau) - U_j(\tau)]$, where $j = 1,2\ldots N$ denotes the general y - mesh point. When the boundary conditions are taken into account, the system takes tridiagonal form amenable to rapid direct solution. That completes the advancement of the weakly nonlinear, extended Meksyn and Stuart solution by a unit time step.

Passing to the nonlinear model described at the end of Section 2, the unit problem of determining the interactive evolution over a time interval Δt of the mean flow and the wave motions associated with a nonlinear instability as well as its bound second harmonic involves the simultaneous integration of equations (29-a,b,c). In that connection, an implicity, second order accurate scheme, where the time and space derivatives are approximated by centered differences, is used to convert (29-a,b,c) into a system of simultaneous linear equations

$$A_j^n \Phi_{j-2}^{n+1} + B_j^n \Phi_{j-1}^{n+1} + C_j^n \Phi_j^{n+1} + D_j^n \Phi_{j+1}^{n+1} + E_j^n \Phi_{j+2}^{n+1} = f_j^n \qquad (31)$$

where $j = 1, 2 \ldots N$, Φ_j^{n+1} denotes the vector with components $(U_j^{n+1} - U_j^n, \phi_{1j}^{n+1} - \phi_{1j}^n, \phi_{2j}^{n+1} - \phi_{2j}^n)$ to be determined at the general y-mesh point j, and the coefficients A_j^n through E_j^n are 5x5 matrices. When the boundary conditions (viz $\Phi_1^{n+1} = 0 = \Phi_N^{n+1}$) are taken into account, the system of equations (31) takes block pentadiagonal form and thus, becomes amenable to direct solution. The algorithm remains quite stable when the time step Δt is chosen consistent with the condition

$$\max\left[r_j\left(|U|_j^n + \varepsilon|\phi_{1y}|_j^n + \varepsilon|\phi_{2y}|_j^n\right) + \varepsilon\alpha\left(|\phi_1|_j^n + 2|\phi_2|_j^n\right)\right] \frac{\Delta t}{\Delta y} \leq 1$$

where

$$r_j = \frac{\varepsilon\alpha\left[|\phi_{1yy} - \alpha^2\phi_1|_j^n + 2|\phi_{2yy} - 4\alpha^2\phi_2|_j^n\right]}{|U_{yy}|_j^n + \varepsilon\left[|\phi_{1yyy} - \alpha^2\phi_{1y}|_j^n + |\phi_{2yyy} - 4\alpha^2\phi_{2y}|_j^n\right]}$$

approximately describes the ratio between the x- and y-derivatives of the vorticity at the jth mesh point and time t.

4. EVOLVING STRUCTURE OF NONLINEAR UNSTABLE WAVE MOTIONS

We consider the evolution of a temporally developing shear layer. The initial state of motion is characterized, in dimensionless variables, by the mean velocity $U(y,0) = \tanh 2y$, upon which the velocity and vorticity fields attendant to the nearly most unstable eigenmode $\alpha = 0.8892$, $\beta(0) = 0 + 0.3784\ i$ are superposed with $\varepsilon = 0.10$ and $A_1(0) = 0.10$. Two rigid plates located at $y = \pm 3.875$ are assumed to bound the flow, and solutions are determined subject to the attendant boundary conditions.

Analysis of the flow development according to the extended, weakly nonlinear, Meksyn and Stuart model yields the suspicious result that, as time progresses, β_i decreases but A_1 increases (Figure 1) to such an extent that the amplitude $a(t) = \varepsilon A_1(\tau) \exp\left(\int_0^t \beta_i dt\right)$ of the perturbation stream function on the axis $y = 0$ distinctly exceeds the linear prediction $\varepsilon A_1(0) \exp(\beta_i(0)t)$ when $a(t) \gtrsim \beta_i^2(0)$ (Figure 2). Whereas this prediction differs from that of the nonlinear model (Figure 2), as well as from the trends suggested by measurements in transitional mixing layers forced at the most unstable frequency (Figure 3), a failure of the Meksyn and Stuart approach is indicated. A little diagnostics readily locates the source of the difficulty in the assumption of slow time variation: even at the initial time the derivative $(\zeta_{1yy} - \alpha^2\zeta_1)_\tau$ is of order unity, much larger than $\zeta_{1\tau}$ (Figure 4).

The trend of $(\zeta_{1yy} - \alpha^2\zeta_1)_\tau$ versus y shown in Figure 4 further suggests that the problem stems from an inadequate description of the vorticity transports in the cat's eye of the evolving wave around the critical layer $y = 0$. In that region, having time dependent lateral extent $\delta(t) \simeq [\varepsilon A_1(\tau) \exp(\int_0^t \beta_i dt)/U_y(0,\tau)]^{1/2} = [a(t)/U_y(0,\tau)]^{1/2}$, the mean velocity U as well as the curvature

of the mean velocity profile U_{yy} are $o(\delta)$; however, by virtue of (12-b) and (14), the time rates of change of those quantities when $\alpha U_y(0,\tau)\delta(t) \geq \beta_i(\tau)$ become respectively, $\beta_i^{-1}U_t \simeq o(\delta^3)$ and $\beta_i^{-1}U_{yyt} = o(\delta)$. Under those conditions the curvature U_{yy}, which has a profound influence on the shape of the eigenfunction ζ_1, exhibits in the critical layer a normalized rate of change $(\beta_i U_{yy})^{-1} U_{yyt} = o(1)$ comparable to that of the disturbance vorticity, viz $[\beta_i(\zeta_{1yy} - \alpha^2\zeta_1)]^{-1} (\zeta_{1yy} - \alpha^2\zeta_1)_t = o(1)$. As a consequence, the assumption that the structures of the mean flow and of the vorticity field associated with the instability vary on a slow time scale collapses, and the weakly nonlinear model fails to describe the flow realistically. The extent of such failure is vividly demonstrated in Figure 5, where the structures of the wave motion predicted by the extended Meksyn and Stuart model and by the nonlinear model for $t = 9.82, a(t) = .285, \beta(\tau) = .1767$ are compared with each other as well as with the structure prevailing at $t = 0$. Even greater divergences arise in a comparison between the growth rates and the structures of the wave motion predicted by the two models for the second harmonic, i.e., the normalized $\zeta_2(y,\tau)/\mathrm{Re}[\zeta_2(0,\tau)]$ and its derivatives vis a vis the normalized $\phi_2(y,t)/\mathrm{Re}[\phi_2(0,t)]$ and its derivatives. Thus, reliance on the nonlinear model is indicated, and justified below, for the problem on hand.

The evolving structure of the wave motion which the nonlinear model predicts for the amplifying instability up to the time of its saturation ($t \lesssim 13.5$ in Figures 2 and 6) compares favorably with experiments on at least two counts. First is the qualitative agreement of the relative growth rate trends predicted by the model for the scaled energies

$$E_{tn}(n\alpha,t) = \int_{-y_w}^{y_w} \frac{\varepsilon^2}{2}(|\phi_{ny}|^2 + n^2\alpha^2|\phi_n|^2)\, dy$$

of the dominant fundamental (n=1) and its second harmonic (n=2) in the time developing shear layer identified at the beginning of this section(Figure 6) vis a vis the relative trends of the energies

$$E_{un}(n\beta,x) = \int_{-y_w}^{y_w} \frac{u'_{r.m.s.}(n\beta,x,y)}{2\theta_m(x_o)\,\bar{u}_I^2}\,dy$$

measured by Miksad (1972) in a space developing transitional mixing layer forced at the same scaled frequency (Figure 3): in both cases the energy of the harmonic grows at a rate approximately 1.5 times that of the fundamental, a behavior certainly not predicted by weakly nonlinear theories. We postpone analysis of this behavior, anticipated qualitatively by Robinson (1974) and discussed further below, to elaborate the second count, viz. the quantitative agreement between the magnitudes of the energies E_{t1} and E_{u1} which theory and experiments, respectively, associate with the fundamental at saturation. Upon reference to the scales of the equivalent temporally developing mixing layer, we set $\theta_m(x_o) = 1/4$ and $\bar{u}_T = 2$ in the definition of E_{u1}. We then proceed to calculate the ratio (E_{t1}/E_{u1}) consistent with these values and with the theoretically predicted structure of the wave motion at saturation. The result is $(E_{t1}/E_{u1}) = 3.5$, a value nicely recovered upon comparison of Figures 3 and 6.

From figures 3 and 6 we also see that the energies E_{t2} and E_{u2} associated with the second harmonic compare favorably during the early phases of development, but depart from each other as the fundamental approaches saturation. A spurious double hump arises in the theoretical predictions at that stage. We discount the significance of the hump feature in the assessment of the nonlinear model on three counts, namely: i) the energy associated with the harmonic remains small compared to that of the fundamental and exhibits

growth/decay trends apparently controlled by the evolution of the fundamental interacting with the mean flow (Figure 3); ii) the qualitative agreement between the results of Zabusky and Deem (1971) and those of Miura and Sato (1978) confirms the secondary impact of the harmonic upon the saturation and post-saturation evolution of the fundamental, i.e., on the processes which underlie the subharmonic generation mechanism proposed and addressed in this paper; iii) the double hump feature, which repeatedly arises in calculations using a truncated Fourier series representation of nonlinear wave motions approaching saturation (see section 5), is eliminated in unsteady twodimensional flow simulations, which do not introduce the truncation approximation (see Zabusky and Deem 1971). Thus, truncation and the attendant neglect of the higher harmonics are responsible for the observed divergence between the energies E_{t2} and E_{u2}; however, the approximation does not obscure the essential aspects of nonlinear instability evolution evidenced by the calculations and indirectly confirmed by the experiments as discussed below.

The prime aspect of finite amplitude instability dynamics resides in the previously noted, relatively rapid, evolution of the curvature U_{yy} of the mean velocity profile within the critical layer of lateral extent $\delta(t)$. We have indicated that U_{yy} undergoes rapid change when and if the nonlinear instability attains a small, but finite, amplitude a(t) such that $\alpha\, U_y(0,\tau)\, \delta(t) \geq \beta_i(\tau)$; conversely, the test $\alpha\, U_y(0,\tau)\, \delta(t) < \beta_i(\tau)$ defines the conditions under which weakly nonlinear models may be employed to realistically describe the structure of the unstable wave motion. Beyond that threshold equations (13) and (14) show that the overall flow evolution becomes characterized by a time rate of change of mean flow vorticity within the critical layer $\beta_i^{-1} U_{yt} = o(\delta^2) = o(a(t))$ comparable to that of the disturbance amplitude $\beta_i^{-1}(da/dt) = a(t)$, but a time rate of change of the y-derivative of mean flow vorticity $\beta_i^{-1} U_{yyt} = o(\delta)$

larger than either of those two within the critical layer. Clearly, the total vorticity $\nabla^2\tilde{\psi}$ in that layer is then described by

$$\nabla^2\tilde{\psi}(x,y,t) = U_y(0,0) + a(t)\,\Omega_i(x,Y,t) \tag{32}$$

where Ω_i denotes a function which is of order unity together with its Y-derivative with respect to the stretched coordinate

$$Y = [U_y(o,t)/a(t)]^{1/2}\quad y = (y/\delta) \tag{33}$$

across the critical layer centered at $y = 0$. If the considered instability, characterized by

$$\varepsilon\psi(x,y,t) \approx a(t)\quad [\cos\alpha x + o(\delta)]$$

in the neighborhood of $y = 0$, dominates the disturbance field, the velocities within the critical layer $Y = o(1)$ are to leading order

$$u = U_y(0,t)\,Y\delta \tag{34-a}$$

$$v = a(t)\,\alpha\sin\alpha x \tag{34-b}$$

Conservation of vorticity then requires that the function Ω_i defined by (32) satisfy the equation

$$\Omega_{iT} + Y\Omega_{i\xi} + \sin\xi\,\Omega_{iY} + \mu_1[\Omega_i - (1 + \frac{\mu_2}{\mu_1})\frac{Y}{2}\quad \Omega_{iY}] = 0 \tag{35}$$

in "boundary layer" coordinates (ξ,Y,T) defined by

$$\xi = \alpha x,\qquad Y = (y/\delta),\qquad dT = (a\alpha/\delta)dt \tag{36}$$

the quantities

$$\mu_1(T) = [d\log a\,(T)/dT] = \beta_i[\alpha^2 a(T)\,U_y(0,T)]^{-1/2} = \beta_i[\alpha U_y(0,T)\delta]^{-1} \tag{37-a}$$

$$\mu_2(T) = -\,[d\log U_y(0,T)/dT] \tag{37-b}$$

being of comparable magnitude < 1 under the considered conditions $(\beta_i/\delta) < 1$.

Inspection of (35) readily suggests that, due to the vorticity transport $\sin\xi\ \Omega_{iY}$, the form of its solution, periodic in ξ over the wavelength 2π of a dominant monochromatic input disturbance, is necessarily

$$\Omega_i(\xi,Y,T) = \Omega_i^{(0)}(Y,T) + 1/2[\sum_{h=1}^{\infty} \Omega_i^{(n)}(Y,T)\, e^{in\xi} + c.c.] \qquad (38)$$

even though $\Omega_i^{(n)}(Y,0) = 0$ for $n \geq 2$. Thus, harmonics are forced by the noted transport within the critical layer. Substitution of (38) into (35), and inspection of the attendant equations for the functions $\Omega_i^{(n)}(Y,T)$, readily show that the forced vorticities $a(T)\,\Omega_i^{(n)}(Y,T)$, $n \geq 2$, become of order $a(T)$ after time intervals $T = o(1)$ and, by that process, harmonic perturbation velocities of order $a^{3/2}(T)$ are generated at the edges of the critical layer. Accordingly, harmonics observed in experiments and determined in nonlinear calculations should exhibit amplification rates approximately 1.5 times as large as that of the dominant fundamental. This is, in fact, the trend evidenced by the results of Figures 3 and 6, and, more generally, by Miksad's (1972) observation that "the measured growth rates of harmonic modes range from 1.15 to 1.73 times that of the fundamental" in transitional mixing layers monochromatically forced at various scaled unstable frequencies. The scatter of the observed growth rate ratios about the value 1.5 is not surprising because different histories of the parameters $\mu_1(T)$ and $\mu_2(T)$ pertain to different situations; accordingly, the components $\Omega_i^{(n)}(Y,T)$ of the solution (38) vary from case to case and so do the ratios between pairs of attendant forced perturbation velocities and energies.

The important role of nonlinear vorticity transports within the critical layer in determining the behavior of finite amplitude instabilities and associated harmonics was recognized by Robinson (1974) who, in fact, proposed an asymptotic

solution to a reduced form of equation (35). In that context, Robinson reached several perplexing conclusions, which contrast with experimental evidence and, thus, warrant specific comment. At issue, are the conclusions that: i) the temporal growth rate of instabilities with wavenumber close to the marginal value 1 for a tanhy mean velocity profile should be $c_i = -3(\alpha - 1)$ instead of $c_i = -0.637(\alpha - 1)$ as predicted by linear theory and indicated by experiments (Miksad 1972), at least in the early phases of nonlinear amplification; ii) no spatially amplifying solutions should exist in the nonlinear range even though data, such as those of Figure 3, clearly display their presence; iii) the harmonics, forced by the nonlinear redistribution of vorticity within the critical layer, should amplify at a rate exactly 1.5 times as large as that of the dominant fundamental, rather than the varying, although comparable, rates noted and rationalized above. Rejection of these conclusions is suggested by the following critical review of Robinson's solution.

A change of independent variables from (ξ, Y, T) to $(\xi, \tilde{\Psi}, T)$, where

$$\tilde{\Psi} = \frac{Y^2}{2} + \cos \xi$$

denotes a scaled stream function in the critical layer, reduces (35) to the equation

$$\Omega_{i_T} + Y\Omega_{i\xi} + \mu_1 \left[\Omega_i - \left(1 + \frac{\mu_2}{\mu_1}\right)\frac{Y^2}{2}\ \Omega_{i\tilde{\Psi}}\right] = 0 \qquad (39\text{-a})$$

In turn (39-a) reduces to the equation (4.28) of Robinson, namely

$$Y\Omega_{i\xi} + \mu_1 \left(\Omega_i - \frac{Y^2}{2}\Omega_{i\tilde{\Psi}}\right) = 0 \qquad (39\text{-b})$$

under the assumptions/approximations that

$$\alpha \simeq 1,\ U_y(0,T) \simeq 1,\ \mu_2(T) = \Omega_{iT}(\xi, \tilde{\Psi}, T) = 0$$

whereupon the parameter $\mu_1 = c_i A^{-1/2}$ in his notation. Robinson determined an asymptotic solution to the reduced equation (39-b) for $\mu_1 << 1$ subject to the boundary conditions that, as $\bar{\psi} \to \infty$, the vorticity Ω_i matches a time invariant mean vorticity distribution upon which is superposed the vorticity of a linear instability having a time invariant wave motion as well as a time invariant amplification rate β_i. Clearly these boundary conditions do not describe the actual state of affairs for even the weakly nonlinear Meksyn and Stuart model predicts that neither the mean flow vorticity (Figure 7) nor the structure (Figure 5) and amplification rate (Figures 1 and 2) of the unstable wave motion remain time invariant outside the critical layer. In fact, Robinson's results contradict the assumed asymptotic behavior for they reveal a velocity jump of order $a^{3/2}(T)$ across the critical layer, a jump which is assumed to be absorbed by the unspecified, and unfortunately neglected, "(a) spreading or contraction of the basic flow, (b) similar spreading or contraction of the fundamental disturbance," as well as by the introduction of all higher-harminics outside the critical layer.

The inadequate boundary conditions lead to an asymptotic solution for $\Omega_i(\xi,Y,T)$ which, according to Robinson's equation (4.48), is completely defined by the instantaneous value of the parameter $\mu_1(T)$, independent of initial conditions and/or previous evolution of the disturbance. Whereas this behavior is incompatible with the indications of either nonlinear models or experiments -- which unequivocally show an influence of prior history upon the evolving structure of nonlinear unstable wave motions -- the particular nature of Robinson's solution, as well as the resolution of the perplexing conclusions it leads to, become apparent. In connection with the conclusion i) we note that the redistribution of vorticity within the critical layer of an evolving nonlinear instability must

be determined by solving equation (35), where the time derivative Ω_{1T} is retained, and not the Robinson's equation [(30-b) in this paper], where Ω_{1T} is neglected. Retention of the time derivative allows the structure as well as the amplification rate of a nonlinear instability with initially small amplitude at first to follow, and then to depart from, the predictions of linear theory. In connection with the conclusion ii) we note that the strong interaction between, and the concurrent evolution of, the mean flow and the wave motion structures require that a realistic description of the spatially developing twodimensional mean flow be recognized and included in the derivation of the vorticity conservation equation within the critical layer of spatially amplifying nonlinear instabilities. Solutions exhibiting spatial amplification, fixed temporal frequency, but gradually varying wavelength, may be gleaned, albeit laboriously, for such an equation -- but not for equation (35), which is predicated on the assumption of streamwise homogeneous mean flow. Finally, in connection with the conclusion iii) we suggest that Robinson's prediction of a fixed value for the growth rate ratios of the harmonics stems from the local similarity character of his solution, only dependent on the instantaneous value of the parameter μ_1. Experimentally observed growth rate ratios scatter around that value because the actual harmonic forcing process, described in a previous paragraph, does not obey local similarity.

Aside from the controversial conclusions discussed above, the crucial shortcoming of Robinson's model resides in the poor comparison between its predictions and those of nonlinear models for the vorticity distributions associated with nonlinear instabilities undergoing saturation and subsequent modulation. Due to the unique dependence of Robinson's solution upon the parameter μ_1 the comparison becomes especially strained at those post-saturation stages in

the actual modulational evolution of the instability where μ_1 has the same modulus, but opposite sign (e.g. t≈ 19.15 vis a vis t = 25.7 in Figure 2); as a consequence, the modulation itself is not predicted. Whereas that process is central to the cyclic mechanism of subharmonic generation and vortex pairing proposed in this paper, solutions of equation (35), subject to appropriate time dependent boundary conditions, are prerequisite to a realistic description of the vorticity redistribution within the critical layer of a nonlinear instability. Unfortunately, such solutions are necessarily numerical and rather laborious, as they require the parallel consistent determination of the matching, slowly varying, outer flow. Unified numerical analysis of the critical layer and the outer flow by a fully nonlinear model proves more economical in practice and, therefore, is adopted here. That consideration notwithstanding, the inner/outer layer view of nonlinear instabilities is useful in that it exhibits the vorticity redistribution mechanism operative within the critical layer as well as the limiting/dominant influence of that process upon the growth of the instability and the forcing of the harmonics.

The conclusion, repeatedly suggested above,that only nonlinear models -- which do not assume either local similarity or self-preservation of the wave motion structure -- realistically describe the evolution of nonlinear instabilities, is also supported by an examination of the approximate model suggested, but not applied, by Miura and Sato (1978). This model assumes that the evolving structure of a temporal instability having wavenumber α may be approximated by (see Equations (3.11) and (3.13) of Miura and Sato 1978)

$$\varepsilon\, \phi_1(y,t) = 2A(t)\, f(y) \exp\,[i\theta(t)\, g(y)] \qquad (40)$$

and that the attendant harmonics may be neglected. Substitution of (40) into (29-a,b) then yields

$$U(y,t) = U(y,0) + 2\alpha(f^2g')'\int_0^t A^2\theta dt$$

(see equations (3.20) of Miura and Sato 1978) as well as two nonlinear ordinary differential equations for A(t) and θ(t), which follow upon formal integration of the real and imaginary parts of (29-b) over the width of the flow (see equations (3.14) and (3.17) of Miura and Sato 1978). The stipulation (40) clearly implies that the wave motion structure retains invariant spatial dependences f(y) and g(y) for the amplitude and phase functions, respectively. The results of Figure 5a support this approximation for times $t \leq 13.5$, prior to saturation; and, in fact, an integration of the equations for A(t) and θ(t) -- with coefficients based on functions f(y) and g(y) determined by the eigenmode structure at t = 0 -- yields reasonable predictions for the presaturation behavior (Figure 2), as well as the saturation time and amplitude, of the test case instability repeatedly discussed in this section. Unfortunately,as shown in the next section, the assumption of invariant spatial dependences, collapses at later times. As a consequence, our solutions, employing the approximate equations derived from (40), fail to reproduce the postsaturation oscillations in wave amplitude and structure, which Miura and Sato claimed to extract, but did not calculate, from their approximate model. Our central interest in those oscillations, vividly displayed by Miura and Sato's own solution of equations (29-a,b) as well as by more elaborate models (e.g., Zabusky and Deem 1971, Patnaik et al 1976), motivates our complete reliance on the nonlinear model for the following study of the vortex pairing mechanism.

5. NONLINEAR MECHANISM OF SUBHARMONIC EXCITATION AND AMPLIFICATION

As noted in previous sections of the paper, measurements of time-averaged properties as well as fluctuation spectra in forced and unforced, transitional and turbulent, statistically stationary, spatially developing mixing layers indicate that, at least for those situations where the forcing frequency is smaller than the most unstable frequency at the initial station, the specific spectrum of disturbances initially coupled to the flow has a vanishing influence on the development of the flow downstream of the station where two or more vortices first agglomerate (Wygnanski et al 1979b, Ho and Huang 1980). Following that event, the spatial growth rate of the forced mixing layer thickness becomes essentially the same as that of the unforced layer characterized by the same velocity ratio $\lambda = (U_1 - U_2)/(U_1 + U_2)$. The finding is significant in that it associates a specific physical event -- one ore more agglomerations -- with the traditional observation that, following some initial relaxation distance, unforced mixing layers tend to grow at a constant rate, which depends on the velocity ratio λ, but is insensitive to the specific initial conditions, transition tripping device and environment of small amplitude random external disturbances encountered in any one experiment.

Whereas the constant growth rate of the self preserving unforced mixing layer is paced by a cyclic process of vortex pairing over statistically averaged lengths which scale with the local layer thickness δ_ω and the velocity ratio λ, the rapid onset of the same dominant process in forced mixing layers strongly suggest that, after the first agglomeration, the history of the large-scale structures/vortices becomes governed by a self-reproducing limit cycle of nonlinear instabilities, viz the cycle already described in Section II in the

course of introducing and justifying the nonlinear model used in the present paper. The key features of the cycle, which we seek to analyze and demonstrate here, are: i) the self-induced modulation of the nonlinear instability responsible for an agglomeration of vortices in the mixing layer combines with the concurrent distortion of the mean flow to provide intrinsic excitation of subharmonic, spatially amplifying, instabilities having about half the frequency of, but nearly the same phase velocity as, the self-modulating wave, hereafter identified as the fundamental; ii) the initial finite amplitude, phase and structure of the subharmonic wave motion produced by the modulation of the fundamental - independent of either local or previous random external forcing at the appropriate frequency -- are conducive to nonlinear amplification of the subharmonic, which draws energy from the fundamental as well as from the mean flow; iii) because of the specific phase relationship between the fundamental and the amplifying subharmonic, pairs of vortices, previously generated by the fundamental, merge with the consequence that the fundamental becomes essentially extinct, while the subharmonic becomes dominant; iv) due to this predominance and to the self-limiting nature of the subharmonic growth -- necessarily bounded by the finite amount of vorticity available to the wave within its fixed wavelength -- specific structures of the mean flow and of the wave motion evolve at subharmonic saturation, viz structures which are conducive to the self-preserving repetition of the instability cycle because they reproduce, except for a doubling of the length scales, the state of motion prevailing at the earlier time of fundamental saturation.

Representative time dependent structures of the mean flow and of the wave motion, which evolve upon saturation of a dominant finite amplitude instability, are illustrated in Figures 2, 6, 8 and 9, which display the long time evolution

($t \gtrsim 13.5$) of the specific, temporally developing, shear layer discussed in Section 4, viz the flow, bounded by rigid plates at $y_w = \pm 3.875$, which evolves from the initial mean velocity field $U(y,0) = \tanh 2y$ and the superposed unstable eigenmode with $\alpha = 0.8892$, $\beta(0) = 0 + -.3784i$, $\varepsilon = 0.1$, $\phi_1(0,0) = 0.1$, under the assumption that the motion remains at all times spatially periodic with wavelength $(2\pi/\alpha)$. Clearly the vorticity distribution achieved at the time when the instability first saturates is not in dynamic equilibrium for the mean as well as the wave motions undergo subsequent structure/amplitude modulations with period $T_{mu} \simeq 17$, about 2.4 times as long as the period $T_f \simeq 7.06$ of the considered instability propagating with phase velocity $c_p = 1$ in the mean flow of initial velocity profile $U(y,0) = (1 + \tanh 2y)$. Although periodic, the noted modulations are not strictly sinusoidal: for example, Figure 2 shows that the stationary value of the y-derivative of the phase function on the axis $y = 0$

$$\Theta_{1y}(0,t) = \{(\partial/\partial y) \tan^{-1}(\mathrm{Im}[\phi_1(y,t)]/\mathrm{Re}[\phi_1(y,t)])\}_{y=0}$$

occurring at $t \simeq 19.15$ precedes the zero of the same function (and the concurrent minimum of the disturbance energy) occurring at $t \simeq 22$ by a time interval $\Delta t \simeq 2.85$, which corresponds to a period $T_{mL} \simeq 11.4$. Thus, the modulation encompasses a band of frequencies centered around $4\pi/(T_{mu} + T_{mL}) = 2\pi/T_{ma}$, where $T_{ma} \simeq 14.2$. Since the period $T_{ma} \simeq 2\,T_f$ almost exactly, the frequency spectrum of the self-modulating wave motion in the flow characterized by the initial mean velocity $U(y,0) = (1 + \tanh 2y)$ would then exhibit - in additon to discrete peaks at the frequencies $(2n\pi/T_f)$ of the dominant wave ($n = 1$) and its harmonics ($n > 1$) - a band of width $\pm 0.2\ (\pi/T_f)$ centered at the frequency (π/T_f) of the 1/2 subharmonic. Interestingly enough, the excitation of just such a frequency band is displayed by the spectral measurements made

downstream of the station where the fundamental saturates in a transitional mixing layer forced at the most unstable frequency (see Miksad 1972, Figure 8, $x \geq 11.5$) Since an approximate doubling of the wavelength relative to that of the fundamental is inherent to the subharmonics observed in the experiments, but not to the modulation of the time-developing shear layer considered in the calculations, some reflection on the stipulated equivalence between temporally and spatially developing flows is in order.

For simplicity of discussion, the relatively narrow band of modulation frequencies exhibited in Figures 2, 6, 8 and 9 is compressed into the central 1/2 subharmonic with strictly trigonometric time dependence. Accordingly, the structure of the temporally developing flow at times $\bar{t} = (t - t_s) \geq 0$ (where $t_s = 13.5$ corresponds to saturation of the fundamental) is approximated by

$$U(y,\bar{t}) = U^{(o)}(y) + \varepsilon[U^{(1)}(y)\, e^{i\pi\bar{t}/T_f} + c.c.] \tag{41-a}$$

$$\varepsilon\phi_1(y,\bar{t})\, e^{i\alpha x} = \varepsilon\phi_1(0,\bar{t})[\phi_1(y,\bar{t})/\phi_1(0,\bar{t})]e^{i\alpha x} =$$
$$\varepsilon\phi_1(0,\bar{t})\tilde{\phi}_1(y,\bar{t})\, e^{i\alpha x} = \varepsilon\{\phi_1^{(o)} + [\phi_1^{(1)}\, e^{i\pi\bar{t}/T_f} + c.c.]\}x \tag{41-b}$$
$$\{\tilde{\phi}_{1c}^{(o)}(y) + i\tilde{\phi}_{1s}^{(o)}(y) + [\tilde{\phi}_{1c}^{(1)}(y)\, e^{i\pi\bar{t}/T_f} + c.c.] + i[\tilde{\phi}_{1s}^{(1)}(y)e^{i\pi\bar{t}/T_f} + c.c.]\}e^{i\alpha x}$$

the complex functions/quantities $U^{(m)}(y)$, $\phi_1^{(m)}$, $\tilde{\phi}_{1c}^{(m)}(y)$, $\tilde{\phi}_{1s}^{(m)}(y)$, $m = 0,1$ being defined by

$$U^{(m)}(y) = (2\varepsilon^m T_f)^{-1} \int_0^{2T_f} U(y,\bar{t})\, e^{im\pi\bar{t}/T_f}\, d\bar{t} \tag{42-a}$$

$$\phi_1^{(m)} = (2T_f)^{-1} \int_0^{2T_f} \phi_1(0,\bar{t})\, e^{im\pi\bar{t}/T_f}\, d\bar{t} \tag{42-b}$$

$$\bar{\phi}_{1c}^{(m)}(y) = (2T_f)^{-1} \int_0^{2T_f} \mathrm{Re}[\bar{\phi}_1(y,\bar{t})] e^{im\pi\bar{t}/T_f}\, d\bar{t} \tag{42-c}$$

$$\bar{\phi}_{1s}^{(m)}(y) = (2T_f)^{-1} \int_0^{2T_f} \mathrm{Im}\,[\bar{\phi}_1(y,\bar{t})]\, e^{im\pi\bar{t}/T_f}\, d\bar{t} \tag{42-d}$$

Calculations, as well as inspection of Figures 2, 6, 8 and 9, indicate that $|U^{(1)}| = o(1), |\phi_1^{(1)}| < |\phi_1^{(o)}|$, $|\bar{\phi}_{1c}^{(1)}| \simeq o \simeq |\bar{\phi}_{1s}^{(o)}|$ and $|\bar{\phi}_{1s}^{(1)}| < |\bar{\phi}_{1c}^{(o)}|$ for the problem on hand. Thus, if only terms of first order are retained in the modulation function/quantities characterized by the superscript m = 1, the stream function $\bar{\psi}^{(t)}$ descriptive of the time developing flow in the domain $\bar{t} \gtrsim o$ may be cast in the form

$$\bar{\psi}^{(t)}(x,y,\bar{t}) = \Psi(y) + \varepsilon\psi(x,y,\bar{t}) = \int_{-y_w}^{y} U^{(o)}(y)\, dy + \frac{\varepsilon}{2}\{2\int_{-y_w}^{y} U^{(1)}(y)dy e^{i\beta_r\bar{t}/2} + \tag{43}$$

$$\sum_{2j=1,2,3} f_1^{(j)}(y) e^{i[\alpha x-(1-j)\beta_r\bar{t}]} + \text{c.c.}\}$$

where $\beta_r = 2\pi T_f^{-1}$ and

$$f_1^{(1/2)}(y) = \phi_1^{(1)*}\, \bar{\phi}_{1c}^{(o)}(y) + i\, \phi_1^{(o)}\, \bar{\phi}_{1s}^{(1)*}(y) \tag{44-a}$$

$$f_1^{(1)}(y) = \phi_1^{(o)}\, \bar{\phi}_{1c}^{(o)}(y) \tag{44-b}$$

$$f_1^{(3/2)}(y) = \phi_1^{(1)}\, \bar{\phi}_{1c}^{(o)}(y) + i\, \phi_1^{(o)}\, \bar{\phi}_{1s}^{(1)}(y) \tag{44-c}$$

This approximate representation, together with the results presented in Section 4, provides the context for examining the structure of the laboratory mixing layer and the applicability of the equivalence in the spatial domains $x_\ell \lesssim x_{\ell s}$ and $x_\ell \gtrsim x_{\ell s}$, which, respectively, correspond to $\tilde{t} \lesssim o$ and $\tilde{t} \gtrsim o$.

The equivalence of temporally and spatially developing flows presumes that the approximate relationship between linear temporal and spatial instabilities established by Gaster (1962) applies as well to the nonlinear flows considered here. Accordingly, the stream function $\tilde{\psi}^{(t)}(x,y,t)$, which describes the evolving structure of the theoretical, monochromatically forced, unsteady shear layer viewed in coordinates (x,y) moving at the phase/group velocity $c_p=c_g=(\beta_r/\alpha)=1$ of the forcing instability with real wavenumber α and complex frequency $(\beta_r+i\beta_i)$ and the stream function $\tilde{\psi}^{(s)}(x_\ell, y_\ell, t_\ell)$, which describes the structure of the experimental, statistically stationary, mixing layer viewed in laboratory fixed coordinates (x_ℓ, y_ℓ) and subject to the spatially amplifying instability with complex wavenumber $\alpha_\ell=\alpha_r+i\alpha_i \simeq \alpha[1+i(\beta_i/\beta_r)]$ real frequency β and nearly coincident phase/group velocities $c_p \simeq c_g \simeq \beta/\alpha_r \simeq 1$, are related by

$$\tilde{\psi}^{(t)}(\alpha x, y, \beta_r t) = \tilde{\psi}^{(s)}(\alpha_r x_\ell - \beta t_\ell, y_\ell, \alpha_r x_\ell) - \int_{-y_{\ell w}}^{y_\ell} (\beta/\alpha_r)\, dy_\ell \qquad (45)$$

when the zero of t_ℓ is chosen so that

$$\tilde{\psi}^{(t)}(\alpha x, y, 0) = \tilde{\psi}^{(s)}(-\beta t_\ell, y_\ell, 0) - \int_{-y_{\ell w}}^{y_\ell} (\beta/\alpha_r)\, dy_\ell$$

However, (45) has a limited domain of validity, as discussed below.

A first limitation to the equivalence becomes manifest upon inspection of the eigenfunctions and eigenvalues calculated in the linear limit: for the initial mean velocity profile U = (1 + tanh2y) considered here, only spatial and temporal instabilities with dimensionless frequency $Re(\beta) \gtrsim 0.8$ approximately satisfy the conditions on wavenumbers, wave velocities and wave motion structures prerequisite to (45). Spatial instabilities which comply with the

equivalence conditions at small amplitudes ($x_\ell \simeq 0$) continue to do so in the process of nonlinear growth and saturation at stations $x_\ell \lesssim x_{\ell s}$. In that domain the phase and group velocities of the spatially amplifying waves remain essentially invariant because the effective wavenumber $\alpha_e(x_\ell) = [\alpha_r\, U_y(0,0)/U_y(x_\ell,0)]$ increases with x_ℓ. The velocity field within the critical layer may then be approximated by

$$u_\ell = (\beta/\alpha_r) + U_y(x_\ell,0)y_\ell \simeq 1 + U_y(x_\ell, 0)y_\ell$$

$$v_\ell = a(x_\ell)\,\alpha_r \sin(\alpha_r x_\ell - \beta t_\ell) + o(a^{3/2})$$

and the vorticity field by

$$\nabla^2\tilde{\psi}^{(s)}(x_\ell, y_\ell, t_\ell) = U_y(0,0)/ + a(x_\ell)\,\Omega_i^{(s)}(x_\ell, Y, \eta)$$

where $\eta = (\alpha_r x_\ell - \beta t_\ell)$ and $\Omega_i^{(s)}$ denotes a function assumed of order unity together with its derivative with respect to the stretched coordinate

$$Y = [U_y(x_\ell, 0)/a(x_\ell)]^{\frac{1}{2}}\, y_\ell = [y_\ell/\delta(x_\ell)]$$

across the critical layer. To a first approximation the function $\Omega_i^{(s)}$ -- which describes the concurrent nonlinear spatial evolutions of the (time averaged) mean flow and the wave motion within the critical layer -- satisfies the equation

$$\Omega_{iX}^{(s)} + Y\Omega_{i\eta}^{(s)} + \sin\eta\,\Omega_{iY}^{(s)} + \mu_1[\Omega_i^{(s)} - (1+\mu_2/\mu_1)\tfrac{Y}{2}\Omega_{iY}^{(s)}] = 0 \qquad (46)$$

in boundary layer coordinates (X, Y, η) defined by $dX = (\alpha_r^2\, a/\beta\delta)dx_\ell$, $Y = (y_\ell/\delta)$, $\eta = (\alpha_r x_\ell - \beta t_\ell)$, the quantities

$$\mu_1(X) = [d \log a(X)/dX],\quad \mu_2 = -[d \log U_y(X,0)/dX]$$

being of comparable magnitude <1 in the domain of nonlinear growth. Equation (46) is formally identical to the equation (35) previously derived for temporally developing shear layers, and so are the attendant initial conditions that $\Omega_i^{(s)}(0, Y, \eta)$ be periodic in η as well as the boundary conditions that for $Y \to \pm\infty$, the velocities and vorticity associated with $\Omega_i^{(s)}(X, Y, \eta)$ match those associated with a mean flow slowly varying in X plus a superposed spatially amplifying weakly nonlinear wave having fixed frequency β and wavenumber α_ℓ that varies slowly with X.. As a result $\Omega_i^{(s)}(X, Y, \eta) = \Omega_i'(T, Y, \xi)$ for $x_\ell < x_{\ell s}$, $\tilde{t} < o$, and equivalence is preserved in those domains.

The equivalence becomes suspect for $x_\ell \geq x_{\ell s}$ because the structure of the laboratory mixing layer predicted by (43) and (45)

$$\tilde{\psi}^{(s)}(x_\ell, y_\ell, t_\ell) = \int_{-y_{ew}}^{y_\ell} [U^{(o)}(y_\ell) + (\beta/\alpha_r)]\, dy_\ell +$$

$$\frac{\varepsilon}{2}\{[f_1^{(\frac{1}{2})}(y_\ell) e^{-i(\beta/2)(t_\ell - t_{\ell s})} +$$

$$2\int_{-y_{ew}}^{y_\ell} U^{(1)}(y_\ell)\, dy_\ell e^{i(\beta/2)(t_\ell - t_{\ell s})}]\, e^{i(\frac{1}{2})(\alpha_r x_\ell - \beta t_\ell)} + \qquad (47)$$

$$f_1^{(1)}(y_\ell) e^{i(\alpha_r x_\ell - \beta t_\ell)} + [f_1^{3/2}(y_\ell) e^{i(\beta/2)(t_\ell - t_{\ell s})}] e^{i(3/2)(\alpha_r x_\ell - \beta t_\ell)} + c.c.\}$$

loses strict time periodicity at the forcing frequency β, while the theoretical time developing shear layer retains spatial periodicity with the initial wavenumber α. In addition to the fundamental -- with fixed amplitude, structure $f_1^{(1)}(y_\ell)$ and frequency β -- (47) indicates the presence of the 1/2 and 3/2 harmonics, with structures subject to a slow time modulation at the frequency $\beta/2$. Linear analysis readily shows that, for the prevailing mean velocity profile $[(\beta/\alpha_r) + U^{(o)}(y_\ell)]$, the 1/2 harmonic constitutes an admissible temporal as well as spatial instability with nearly equal phase and group velocities $c_p \simeq c_g \simeq (\beta/\alpha_r)$ practically coincident with those of the

dominant fundamental, but the 3/2 harmonic does not. The possibility then arises that a time-modulated, or intermittent, excitation of the 1/2 subharmonic instability occur at appropriate downstream stations in a spatially developing mixing layer dominated by a finite amplitude large scale instability as the counterpart to the temporal modulation of the fundamental wave motion. structure in the equivalent temporally developing shear layer. Should the subharmonic instability become amplified, the equivalence between the two flows would clearly be broken.

Linear analysis fails to indicate whether and when the 1/2 subharmonic is amplified because the stream function of the associated, slowly modulated wave motion with real part

$$[\mathrm{Re}(f_1^{(1/2)}) + 2\int_{-y_{\ell w}}^{y} U^{(1)}\, dy_\ell]\cos\tfrac{\beta}{2}(t_\ell - t_{\ell s}) + \mathrm{Im}(f_1^{(1/2)})\sin\tfrac{\beta}{2}(t_\ell - t_{\ell s}) \quad (48\text{-a})$$

and imaginary part

$$\mathrm{Im}(f_1^{(1/2)})\cos\tfrac{\beta}{2}(t_\ell - t_{\ell s}) - [\mathrm{Re}(f_1^{(1/2)}) - 2\int_{-y_{\ell w}}^{y} U^{(1)}\, dy_\ell]\sin\tfrac{\beta}{2}(t_\ell - t_{\ell s}) \quad (48\text{-b})$$

carries little resemblance to that of a linear wave at any time $0 < (t_\ell - t_{\ell s}) < 4\pi/\beta$. This structural difference also prevents the adoption of either Kelly's (1967) theory or its extensions in terms of weakly nonlinear multiple scale models of secondary instabilities (e.g., Nayfeh and Bozatli 1979) to determine the parameteric amplifier action, if any, of the coexistent nondispersive finite amplitude fundamental. Seemingly, the only resort then resides in nonlinear numerical calculations, which in view of the nondispersive nature of the fundamental and the subharmonic at the considered stage of flow development, may be based on the heuristically equivalent, time-developing, nonlinear flow model of equations (29,a,b,c,).

Numerical experiments, involving the integration of (29-a,b,c) subject to the distinct sets of initial conditions which accrue when the mean velocity field and the fundamental wave motion displayed in (47) are combined with the subharmonic wave motions indicated by (48-a,b) for distinct times t_ℓ, indicate that, subject to a variable time delay generally shorter than $(2/\beta)$, nonlinear effects cause the subharmonic to undergo a strong nearly exponential amplification with characteristic time comparable to $(2/\beta)$ for those initial conditions which pertain to times t_ℓ in the interval roughly bounded by $-(\pi/\beta) < (t_\ell - t_{\ell s}) < (\pi/\beta)$.* Since those initial conditions recur with a time period $(4\pi/\beta)$ according to (48-a,b), strong, but intermittent, subharmonic growth is indicated for the region of the laboratory mixing layer which extends approximately $(2\pi/\alpha_r)$ downstream of the station $x_\ell = x_{\ell s}$ where the forcing fundamental saturates. Such a region of intermittent nonlinear subharmonic excitation/amplification -- inherent to the evolution of the fundamental and independent of external forcing at the appropriate frequency -- has been observed by Miksad (1972, p. 714) in transitional mixing layers. Its occurrence and interpretation are quite significant in our view of mixing layer dynamics because they provide the first two elements of the self-reproducing nonlinear cycle of large scale instabilities which we seek to demonstrate.

e nonlinear nature of the subharmonic excitation/amplification process requires that it be analyzed in the context of the concurrent changes in mean flow and fundamental wave motion. The intermittent activity over the noted distance (stream of $x_{\ell s}$ admittedly prevents the exact simulation of that region of the

*A reexamination of the evolving structure of the fundamental wave motion prior to saturation (see Section 4) shows that the stream function $\tilde{\psi}(t)$ is adequately described by the approximation (43) for $\tilde{t} > -(\pi/\beta)$.

laboratory flow by a single, equivalent, time-developing shear layer having the streamwise periodic structure attendant to superposed sinusoidal fundamental and subharmonic waves. However, intuition as well as data (e.g., Figure 3) suggest that only a modest amount of energy accrues to the subharmonic in the region of intermittent activity. An approximate simulation then seems plausible, especially if attention is focused on the flow structure which ultimately evolves upon finite amplitude growth and saturation of the subharmonic. In that connection a station $x_{\ell o}$ is chosen within the region in question downstream of $x_{\ell s}$; non-intermittent activity is assumed to begin at that station, and effective initial structures are prescribed there for the time-averaged velocity profile as well as for the fundamental and the subharmonic wave motions. Given the small energy accrued to the subharmonic, the effective initial structures may not differ substantively from those indicated by (47); accordingly, a parametric study need only consider moderate variations in the partition of energy among the modes and in the structure of the subharmonic wave motion from its time-average during the periods of activity. Limited numerical experiments indicate that such variations have little influence on the ultimate development of the flow. In the absence of a cogent criterion to guide the choice, only the representative results of a single approximate simulation are therefore reported and discussed below; the pertaining initial conditions are: i) $x_{\ell o} = x_{\ell s} + (\pi/\alpha_r)$; (ii) structures of the mean velocity profile and of the fundamental wave motion as displayed in (47); iii) structure of the subharmonic motion as indicated by (47) for $(t_\ell - t_{\ell s}) = 0$.

The structural evolution of the equivalent temporally developing flow, which ensues upon excitation of the subharmonic, is illustrated in Figures 10, 11 and 12. Inspection of these figures elicits several commerts. Clearly the subharmonic amplification and saturation constitute strongly nonlinear processes

accompanied by large changes in the structures of the mean velocity profile as well as the fundamental and the subharmonic wave motions. The salient consequences include: i) the binary merging of the vorticity concentrations generated by the preexisting fundamental which, in fact, transfers most of its energy to the subharmonic as the latter approaches saturation (Figure 12); ii) an increase in the mean flow vorticity thickness δ_ω which, at subharmonic saturation, becomes very nearly double that prevailing at fundamental saturation (Figures 8 and 10); iii) an evolution in the subharmonic wave motion which, consistent with flow self-preservation, acquires at saturation a structure and an energy which are, respectively, equal and double their counterparts in the fundamental wave motion at its saturation (Figures 9,11 and 12); iv) a self-induced modulation of the mean and subharmonic wave motions which follows subharmonic saturation and, consistent with the flow structure and the time/length scales attendant to that event, causes first the intrinsic excitation of a 1/4 subharmonic wave, and then its evolution with a life cycle dynamically identical to that of the subharmonic. In combination these processes complete the demonstration of the proposition that a single self-reproducing cyclic process of 1/2 subharmonic excitation, amplification and quenching controls the evolution of large scale coherent structures as well as mean flow in spatially developing mixing layers.

Disagreement between relevant experimental data prevents a definitive quantitative evaluation of the analytical results for the nonlinear wave cycle. The subharmonic amplification rate displayed in Figure 12 is measurably larger than that reported by Miksad (1972) and reproduced in Figure 3, but agrees nicely with that observed by Ho and Huang (1980, see Figure 17) in mixing layers forced at frequencies slightly below that of maximum amplification. The apparent contradiction may be facility related. Both experiments were carried out in channels with relatively small cross-sections, viz 12.5 x 13.5 cm for an

estimated vorticity thickness $\delta_\omega \simeq 3$ cm at subharmonic saturation in Miksad's case and 10 x 10 cm for $\delta_\omega \simeq 1.2$ cm in Ho and Huang's case. As Miksad points out, cross-stream boundaries then exert spanwise constraints on the three dimensional secondary instabilities with large spanwise wavelength (see Browand and Troutt 1980, Figure 6) which arise in the course of subharmonic amplification, and cause skewing as well as apparent branching of the large scale structures (see Miksad 1972 Figure 24 as well as Browand and Troutt 1980). According to Miksad "the onset of spanwise activity coincides with a noticeable decay of fundamental mode energy along the center-plane"; however," $u'_{r.m.s.}$ wave-front measurements indicate that this may be due to a spanwise redistribution of energy and not to a transfer of energy to other scales of motion." Thus, it is possible that the subharmonic amplification rate measured by Miksad in the center-plane of his facility, with a ratio $(d/\delta_\omega) \simeq 4$ between channel width d and mixing layer thickness δ_ω, may not represent either the spanwise average value or the value appropriate to a flow free of lateral constraints; by contrast, the rate observed by Ho and Huang with $(d/\delta_\omega) \simeq 8$ may not be subject to such adverse limitations. Admittedly this is only a conjecture. However, a stronger argument may be made in support of the calculated results and Ho and Huang's measurements by examing the average spatial growth rate of the mixing layer over the interval between fundamental and subharmonic saturation. For the mean velocity profiles shown in Figure 10 and the considered velocity ratio $\lambda = 1$ we obtain

$$(d\theta/dx) = (d\theta/dt) \simeq (1/4)(d\delta_\omega/dt) \simeq .03$$

a result which scales in the lower range of the experimental observations reported by Brown and Roshko (1974) and Browand and Latigo (1979), if the growth rate of the integral (momentum) thickness θ is assumed to depend linearly on λ. Thus, the the most commonly measured gross feature of mixing layer development is fairly reproduced by the model and calculation presented here.

6. DISCUSSION

The results of section 5 indicate that the growth of spatially developing turbulent mixing layers is controlled by a self-reproducing deterministic, nonlinear wave mechanism whereby sequentially subharmonic, large-scale, finite amplitude instabilities are caused to follow a well defined excitation/amplification/quenching life cycle, which renders them sequentially dominant. The key to the mechanism resides in the strongly nonlinear nature of the interactions between, and the concurrent structural evolutions of, the mean flow and the locally dominant wave motions. The salient consequences of those nonlinearities include: i) the achievement of negligible dispersion between a dominant instability at/near saturation and its 1/2 subharmonic, provided the frequency of the fundamental falls in a range to be discussed below; ii) the onset of non-stationary mean and wave motions upon saturation of the dominant fundamental, and the consequent intermittent excitation of 1/2 and 3/2 harmonic wave motions having well defined structures; iii) the approximate doubling of the mean flow thickness and the near complete draining of the fundamental energy, which accompany the amplification/saturation of the unstable subharmonic and permit the self-preserving reproduction of the (subharmonic) instability excitation/amplification/quenching processes in sequential cycles distinguished only by a sequential doubling of the length of scales involved.

The deterministic and skeletal nature of the proposed cyclical instability mechanism -- ascribing a significant role to a discrete, two frequency, spectrum of two dimensional waves in each cycle -- has distinct implications with regard to the dynamics of turbulent mixing layers and their amenability to control. The quantitative pursuit of these implications is beyond the scope of the present paper; however,some relevant qualitative trends may be gleaned from the

available results. The first comment in this connection concerns the expected behavior of transitional mixing layers monochromatically forced at unstable frequencies β other than the β_m of maximum amplification considered in our calculations. Since the growth of any instability is limited by the finite amount of vorticity available to it within a wavelength, one anticipates that, in accord with the observations of Miksad (1972, p. 712), the saturation amplitude of a forced disturbance increase as its frequency decreases. The mean flow distortion (increase in δ_ω), which accompanies the growth of the instability and is geared to its saturation amplitude, is also expected to increase as the frequency decreases. As a result, conditions conducive to the excitation of a 1/2 subharmonic, having nearly the same propagation velocity as the forcing fundamental, and the attendant initiation of a nonlinear subharmonic generation cycle, may be anticipated for a finite range of forcing frequencies about β_m. The experiments of Ho and Huang confirm this expectation for $(\beta_m/2) < \beta < \beta_m$; the range of admissible frequency $\beta > \beta_m$ remains to be determined by either calculation or experiment.

For a specified initial mean flow, forcing at different frequencies in the aforenoted range results in initial mixing layer responses, hereafter identified as mode 1, which are qualitatively identical, but quantitatively different because each frequency possesses a specific admittance, amplification rate, saturation amplitude and rate of energy transfer to its subharmonic. However, the frequency sensitivity should largely vanish upon the first vortex pairing because the subharmonic responsible for that event, saturated at a self-limiting amplitude consistent with its wavelength, combines with the attendant commensurate distortion of the mean velocity profile to yield a flow structure which, in coordinates scaled to the local mixing layer thickness, is independent of the

initial conditions. If the nonlinear instability cycle proposed here is operative, the development of the flow, downstream of the station where vortex pairing first occurs, should then become self-preserving and independent of the specific transition process, whether forced or natural. This self-preserving behavior, which is the cornerstone of the proposed model, is manifested by the measurements of Ho and Huang (1980) in forced flows, as well as by Broward and Latigo's (1979) observation that, in naturally developing flows subject to distinct initial conditions, the mean velocity distributions achieve an equilibrium shape in coordinates scaled to the local mixing layer thickness after two vortex pairings, and the distributions of rms longitudinal fluctuations as well as Reynolds stress do so prior to the third pairing. Consistency with the proposed mechanism is thus indicated, but not conclusive support. Clearly the suggested predominance of a deterministic two dimensional instability cycle involving a discrete two frequency spectrum must be reconciled with the experimental evidence that mixing layer turbulence is random, three dimensional and broad spectrum. This reconciliation is pursued below following some additional discussion of initial mixing layer responses.

Ho and Huang (1980) point out that the initial response changes at low forcing frequencies $\beta \leq (\beta_m/2)$.* Different modes, designated by $n = 2,3,4$, arise for different frequency ranges $\beta_m/(n+1) \lesssim \beta \lesssim \beta_m/n$. Due to the receptivity and amplification characteristics of the flow, the n^{th} harmonic of the forcing frequency dominates the initial development in mode n. In the higher modes (i.e. $n = 3,4$) the $(n-m) > 1$ harmonics also appear and initially dominate over the forcing

*Attention is here restricted to small amplitude forcing, which has a small influence on the spatial evolution of the instabilities compared to their interactions with the mean flow and with each other. The collective interactions, which sometime arise under large amplitude forcing (Ho and Nosseir 1981), require separate analysis.

frequency; however, their energies and amplification rates remain distinctly smaller than those accruing to the n^{th} harmonic. This "response" frequency then amplifies and saturates along the lines discussed in Section 4, with little interference by the other instabilities simultaneously present in the flow; as it so evolves, it generates vorticity concentrations as well as mean flow distortions, which tend to eliminate the initial differences between the phase velocities of the various instabilities.

According to the considerations set forth in a previous paragraph, the flow distortion attendant to the saturation of the response frequency eliminates the dispersivity of that wave relative to its 1/2 subharmonic, which coincides with the forcing frequency in mode 2. Binary vortex merging then ensues in mode 2, much along the lines repeatedly discussed in this paper, but without the delay required for intrinsic excitation of the subharmonic, which is now forced and amplified ab initio. As the forced subharmonic saturates at its self-limiting amplitude, conditions conducive to self-preserving development of the flow are recovered upon the first vortex pairing. The ensuing development must be the same as that of mixing layers initially responding in mode 1, and that is the case according to the observations of Ho and Huang (1980).

In mode 3 the saturation of the response frequency is also followed by the continued growth of its 1/2 subharmonic, forced and amplified ab initio in the mixing layer. However, that process does not proceed to self-limiting saturation as in mode 2, because the attendant mean flow distortion eliminates the dispersivity of the forcing frequency relative to the response frequency and the 1/2 subharmonic. A three-wave nonlinear interaction then arises, which results in the merging of every triad of vortices generated by the response frequency. Since the rate of energy transfer among the three interacting waves depends upon their phase relationship, the pattern of merging varies from event to event: in most cases two members of the vortex triad

merge first into a new vortex, which then coalesces with the third member; occasionally, all three members merge at the same time. In all cases the waves at the response frequency and its 1/2 subharmonic become largely extinct upon completion of the merging, while the wave at the forcing frequency becomes distinctly dominant, reaching saturation at a self-limiting amplitude consistent with its wavelength. This saturated wave combines with the attendant commensurate distortion of the mean flow to yield a flow structure which, when viewed in coordinates scaled to the local mixing layer thickness, is largely identical to those encountered at subharmonic saturation in modes 1 and 2. Self-preserving development of the flow is then regained downstream of the station where the vortex triad coalesces, in agreement with the observations of Ho and Huang (1980).

The response in mode 4 is qualitatively similar to that in mode 3 to the extent that saturation of the response frequency is followed first by amplification of its 1/2 subharmonic and then by a three-wave interaction with the forced 1/4 subharmonic,which ultimately becomes dominant and saturates at its self-limiting amplitude. Self-preserving development of the flow then ensues downstream of the station where quadruple vortex coalescence is completed, again in agreement with the observations of Ho and Huang (1980). The nonlinear viewpoint and mechanism advanced here thus allow a unified interpretation and description of the processes whereby a mixing layer subject to diverse initial conditions and external forcing relaxes to a self-preserving behavior. The comments below seek to ascertain the role of that mechanism in the fully developed turbulent regime.

In a fully developed turbulent flow, the dominant, large scale instabilities considered here are subject to distinct amplitude and frequency modulations, induced either by externally imposed disturbances or by secondary three-dimensional instabilities intrinsic to the vorticity patterns which evolve with the

large scale structures. Given the nonlinear nature of the instability evolution process, these modulations result in the seemingly random occurrence in time and space of the major observable events, e.g., vortex pairings. Thus, for example, in a naturally transitioning mixing layer, where the initial amplitude and frequency of the selected response disturbance are subject to modulation, the first vortex pairing occurs randomly in time and space mainly because the strength and separation of the participating vortices vary with the modulation of the generating disturbance. As a result, the mean vorticity thickness δ_ω displays linear growth beginning at/about the station where the random pairing occurs in the mean.

In a forced mixing layer, where the initial amplitude and frequency of the response disturbance are determined uniquely, the position of first vortex coalescence (either binary or multiple depending on the response mode) becomes localized. Up to that position, the thickness δ_ω grows in the stepwise fashion predicted, for example, by the strictly twodimensional, deterministic calculations of Aref and Siggia (1980) and this paper. Beyond that position however, the thickness δ_ω grows linearly because secondary instabilities, intrinsic to the vorticity patterns generated by the first coalescence, modulate the amplification of the subharmonic responsible for the second coalescence and cause that event to occur randomly in space and time.

Prominent among the modulating disturbances are the secondary threedimensional instabilities which cause the formation of longitudinal streaks (Miksad 1972, Brown and Roshko 1974), and the spanwise redistribution of the dominant mode energy alluded to in Section 5. Their effect is to impart spanwise-variable rates/stages of evolution/merging upon the vortical structures associated

with the dominant mode at a ground-fixed observation station. The immediate consequences are twofold: I) the evolving structures attain spanwise skewed/branched configurations as observed by Browand and Troutt (1980); II) sequential structure realizations at a fixed observation station exhibit jitter in their phase and amplitude/stage of evolution according to some probability density function (p.d.f.). In the present view the scale relationship, as well as the mode and extent of interaction between the dominant streamwise and spanwise instabilities, are deterministic; randomness is relegated to the spanwise phase exhibited by the latter instability in sequential realizations of the structures at the observation station. Specifically, the spanwise instability embodies the selective response of the supporting vorticity concentration to the random forcing provided by the prevailing three-dimensional disturbance environment. The receptivity and amplification characteristics of the vortical structure with respect to spanwise disturbances act as band pass filters to select the "response". As a result, the wavelength of the spanwise instability necessarily scales with that of the locally dominant streamwise mode and with the related local mean vortical thickness δ_ω of the mixing layer. Upon selection, the spanwise instability grows to an amplitude limited by the nonlinear requirement that the ensuing threedimensional stretching of the supporting vortical structure remain bounded. As a result, the p.d.f. of the structures observed at a fixed station possesses a well-defined finite spread; also, the structures persist and cyclically reproduce themselves with quasi-two dimensional form at large distances downstream. Finally, if the structure generation mechanism and life cycle are self-preserving as proposed in this paper, so must be their interactions with the spanwise instabilities and, therefore, the statistics of structures observed at different downstream stations. The experimental findings that the p.d.f.

of vortical structure lifetime in a mixing layer (Roshko 1976) as well as the spanwise distribution of cross-correlation coefficient (Browand and Troutt 1980) are in fact self-preserving, support this conclusion. Thus, deterministic nonlinear mechanisms and bounds appear to control not only the twodimensional evolution of the structures but also their concurrent seemingly random, finite amplitude, threedimensional modulations and distortions, which are prerequisite to the aforenoted onset of self-preserving behavior, with linearly growing mean thickness, following the first coalescence of vortices in forced as well as unforced mixing layers.

A consequence of the interaction between large scale streamwise and spanwise instabilities, and the attendant jitter of the structures, is the broadening of the low frequency peak in the spectra of fixed point measurements in a turbulent mixing layer. Unfortunately, this broadening does not necessarily control the shape of the low frequency spectrum. The large scale nonlinear waves, which dominate the flow according to the present model, have nonsinusoidal shape (see Section 4) further complicated by the modulations attendant to the jitter. The coherence of such waveforms is easily lost in a spectral representation, which disregards phase information and provides only an averaged linear Fourier decomposition of the signal. For thesignal shapes on hand the Fourier decomposition typically includes several artifacts which further broaden the spectrum (Lake and Yuen 1978). Thus, the proposed dominant wave model of mixing layer dynamics is not contradicted by the absence of spectral peaks in the large body of accepted measurements within turbulent mixing layers.

An additional noteworthy aspect of the interaction between the large scale streamwise and spanwise instabilities in a mixing layer becomes manifest upon a comparison of the mean thickness growth rates measured in experiments with those predicted by deterministic, strictly two-dimensional models, which ignore the spanwise instability (e.g. Aref and Siggia 1980 as well as Section 5 of this paper). Remarkably, theory and observation are in reasonable agreement, thus indicating a null average effect of the interaction upon the development of the flow. Several additional inferences may then be advanced. First of all, the twodimensional models adequately describe the distribution of Reynolds stress in the flow. Conversely, Reynolds stress distributions so predicted provide a first principle alternative and/or complement to flow analysis by the generally accepted second order closure models, whose success often depends on the suitable empirical selection of third order correlation coefficients. Secondly, the cascade of energy in threedimensional wavenumber space provides an important contribution to the level and distribution of turbulent kinetic energy in the flow, but has little influence, either qualitative or quantitative, on the evolution of the large scale structures and on the distribution of Reynolds stress. Since the distributions of all second order turbulence quantities in a mixing layer become self-preserving after the second vortex pairing (Browand and Latigo 1979) *, the cascade must be intrinsic to, and bound with, the evolving vorticity patterns of the large scale structures, and must evolve subject to the same broad constraints previously indicated

* We conjecture that the low frequency and inertial subranges of spectra become also self preserving after the second vortex pairing.

for the large scale spanwise instability -- i.e., wave vectors selected by the receptivity and amplification characteristics of the supporting advected flow patterns, phase determined case by case by the prevailing random disturbance environment, amplification limited by nonlinear bounds on the ensuing distortion of the supporting flow patterns, effect confined to localized distortions of the dominant carrier waveshape and the associated distributions of fluctuations. The overall energy of the carrier wave and its evolutionary interaction with the mean flow are then influenced only slightly, and the self-preserving statistics of the cascade process, as well as its negligible effect upon the dynamics of the large scale structures and the development of the flow, are rationalized.

The arguments above support the premise of the proposed model that the large scale structures and the mean flow of a mixing layer constitute a largely self-contained nonlinear twodimensional flow system, which evolves by a self-reproducing deterministic limit cycle. The cycle, although subject to modulation by intrinsic self-limiting instabilities, becomes rapidly oblivious of initial conditions. Control of the flow then seems possible only by repeated local interference with either the mean flow or the dominant modes associated with the large scale structures. For example, one anticipates that, in line with the findings of Ho and Huang (1980), the growth rate of the mean mixing layer thickness at a selected downstream distance is enhanced by in phase, small amplitude, external, forcing of either the locally dominant wave frequency or its nondispersive fractional subharmonics. Conversely, one expects that the growth rate is diminished if the frequency of the forcing is preserved, but its phase is reversed. Receptivity considerations together with the proposed model, and/or slight extensions thereof,

should provide a realistic tool for evaluating the effectiveness of such control concepts and for designing attendant demonstration experiments.

This work was supported by the Office of Naval Research under Contract N00014-79-C and, in part, by the Office of Scientific Research under Grant AFOSR 80-0184.

REFERENCES

Acton, E. 1976 The modeling of large eddies in a twodimensional shear layer. J. Fluid Mech. 76, 561-592

Aref, H. and Siggia, E.D. 1980 Vortex dynamics of the twodimensional turbulent shear layer. J. Fluid Mech. 100, 705-737.

Browand, F.K. and Latigo,B.O. 1979 Growth of the two-dimensional mixing layer from a turbulent and non-turbulent boundary layer. Phys. Fluids 22, 1011-1019.

Browand, F.K. and Troutt, T.R. 1980 A note on spanwise structure in the twodimensional mixing layer. J. Fluid Mech. 97, 771-781

Brown, G.L. and Roshko, A. 1974 On density effects and large structure in turbulent mixing layers. J. Fluid Mech. 64, 775-816

Gaster, M. 1962 A note on the relation between temporally-increasing and spatially-increasing disturbances in hydrodynamic stability. J. Fluid Mech. 14, 222-224.

Ho, C.M. and Huang, L.S. 1980 Subharmonics and vortex merging in mixing layers. Submitted to J. Fluid. Mech.

Ho, C.M. and Nosseir, N.S. 1981 Dynamics of an impinging jet. Part 1. The feedback phenomenon. J. Fluid Mech. 105, 119-142.

Kelly, R.E. 1967 On the stability of an inviscid shear layer which is periodic in space and time. J. Fluid Mech. 27, 657-689.

Lake, B. M and Yuen, H.C. 1978. A New Model for NonLinear Wind Waves. Part 1 Physical Model and Experimental Evidence. J. Fluid Mech., 88, 33-62.

Meksyn, D. and Stuart, J.T. 1951 Stability of viscous motion between parallel planes for finite disturbances. Proc. Roy. Soc. A 208, 517-526.

Michalke, A. 1964 On the inviscid instability of the hyperbolic-tangent velocity profile. J. Fluid Mech. 19, 543-556.

Michalke, A. 1965 On spatially growing disturbances in an inviscid shear layer. J. Fluid Mech. 23, 521-544.

Miksad, R.W. 1972 Experiments on the nonlinear stages of free-shear-layer transition. J. Fluid Mech. 56, 695-719.

Miura, A. and Sato, T. 1978 Theory of vortex nutation and amplitude oscillation in an inviscid shear instability. J. Fluid. Mech. 86, 33-47

Nayfeh, A.H. 1973 Perturbation Methods. Wiley, New York, New York, Chap. 6.

Nayfeh, A.H. and Bozatli, A.N. 1979 Secondary instability in boundary-layer flows. Phys. Fluids 22, 805-813.

Patnaik, P.C., Sherman, F.S. and Corcos,G.M. 1976 A numerical simulation of Kelvin. Helmholtz waves of finite amplitude. J. Fluid Mech. 73, 215-240

Petersen, R.A. 1978 Influence of wave dispersion on vortex pairing in a jet. J. Fluid Mech. 89, 469-495.

Robinson, J.L. 1974 The inviscid nonlinear instability of parallel shear flows. J. Fluid Mech. 63, 723-752.

Roshko, A. 1976 Structure of turbulent shear flows: A new look. AIAA J. 14, 1349-1357.

Stuart J. T. 1960 On the nonlinear mechanics of wave disturbances in stable and unstable parallel flows. Part 1. The basic behavior in plane Poiseuille\flow. J. Fluid Mech., 9, 353-370.

Tam, C.K.W. 1978 Excitation of instability waves in a twodimensional shear layer by sound. J. Fluid Mech., 89, 357-371.

Winant, C.D. and Browand, F.K. 1974 Vortex pairing: the mechanism of turbulent mixing layer growth at moderate Reynolds number. J. Fluid Mech. 63, 237-255.

Wygnanski, I., Oster, D., Fiedler, H. and Dziomba, B. 1979a On the perserverence of a quasi twodimensional eddy-structure in a turbulent mixing layer. J. Fluid Mech., 92, 1-16.

Wygnanski, I., Oster, D. and Fiedler, H. 1979b A forced plane turbulent mixing layer: A challenge for the predictor. The Second Symposium on Turbulent Shear Flow, Imperial College, London.

Zabusky, N.J. and Deem, G.S. 1971 Dynamical evolution of twodimensional unstable shear flows. J. Fluid Mech., 47, 353-379.

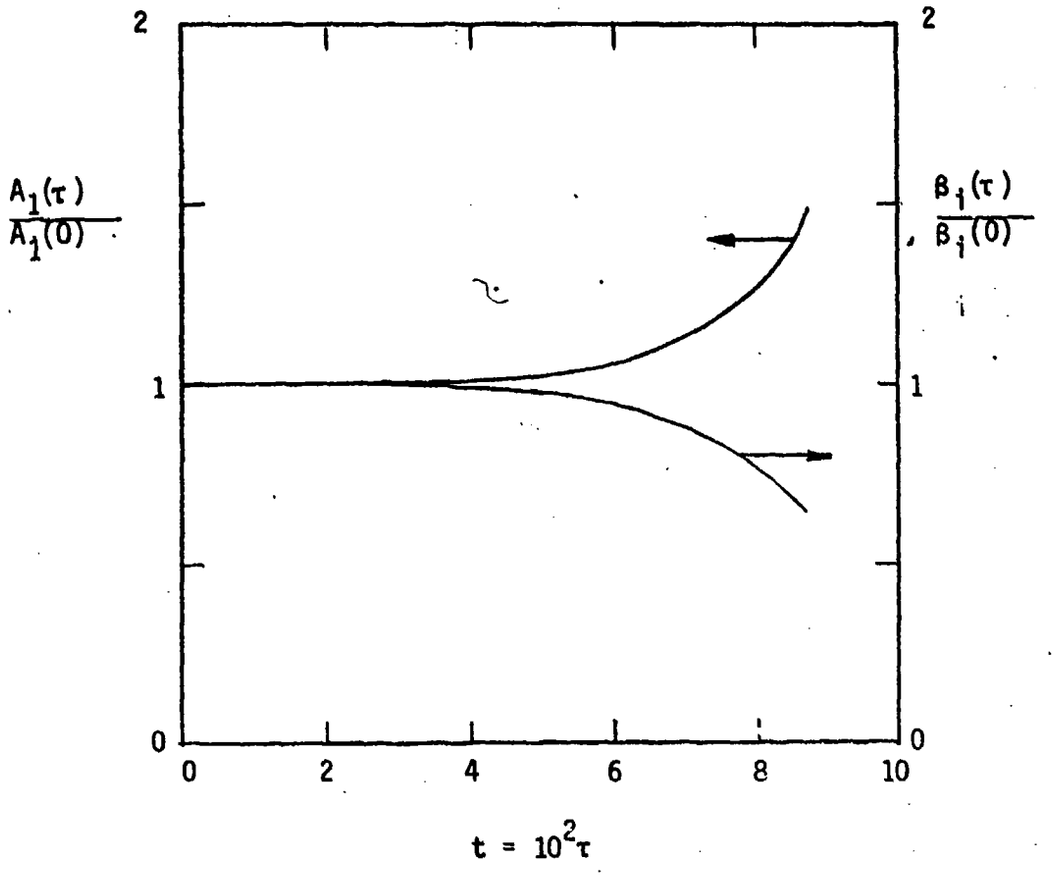

FIGURE 1: The preexponential factor $A_1(\tau)$ and the amplification rate $\beta_1(\tau)$ of the fundamental wave according to the extended Meksyn and Stuart model.

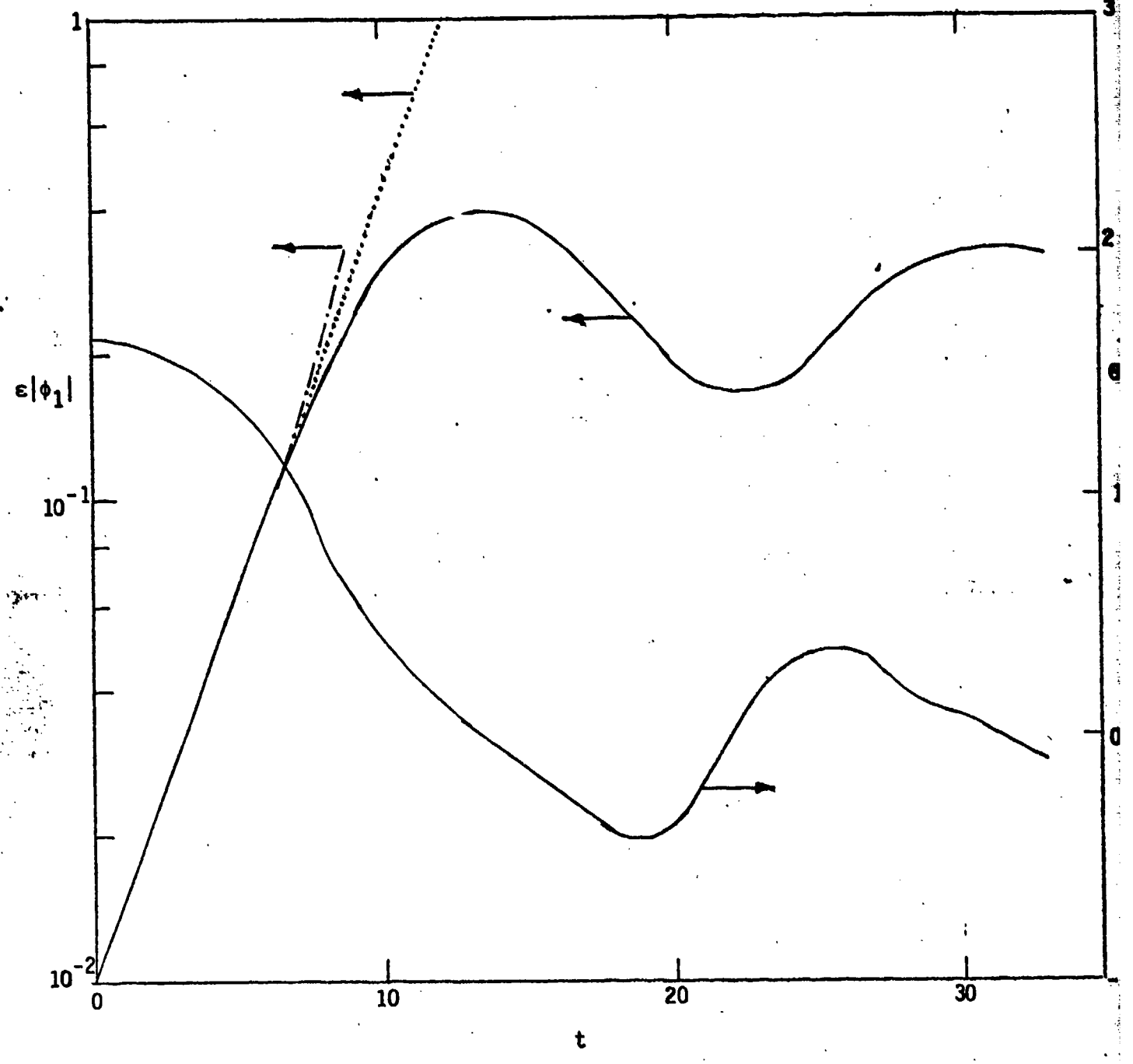

FIGURE 2: The stream function modulus $\varepsilon|\phi_1(0,t)|$ and phase derivative $\theta_{1y}(0,t) = \mathrm{Im}[\phi_{1y}(0,t)]/\mathrm{Re}[\phi_1(0,t)]$ of the fundamental wave motion. ——— Nonlinear model; -·- extended Meksyn and Stuart model; ····· linear model.

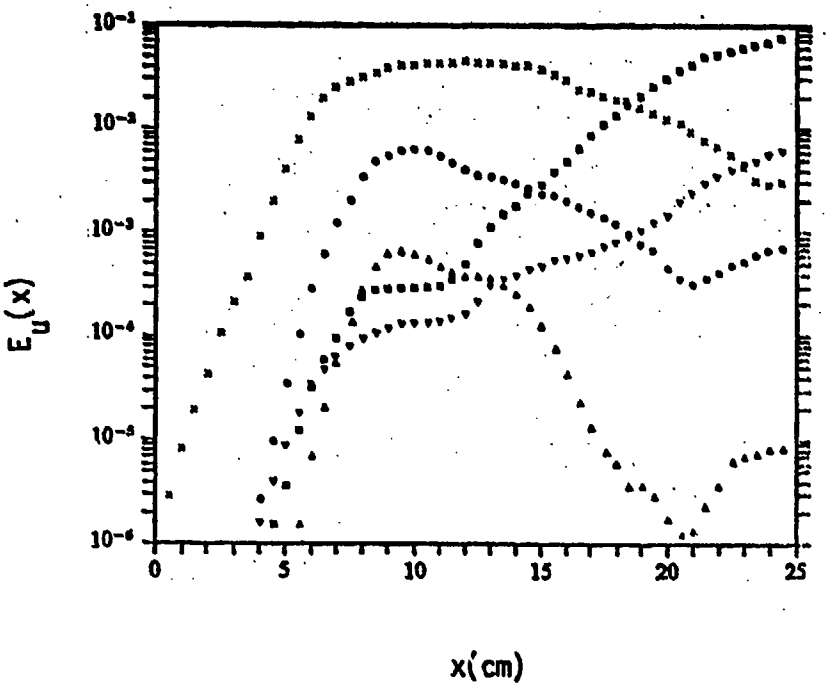

FIGURE 3: Experimentally observed downstream growth of the integrated u' r.m.s. energy of disturbances in a mixing layer forced at the dimensionless frequency $\beta = 0.222$. x, β ; o, 2β; Δ, 3β; $\square$,$(1/2)\beta$; ∇,$(3/2)\beta$. From Miksad (1972).

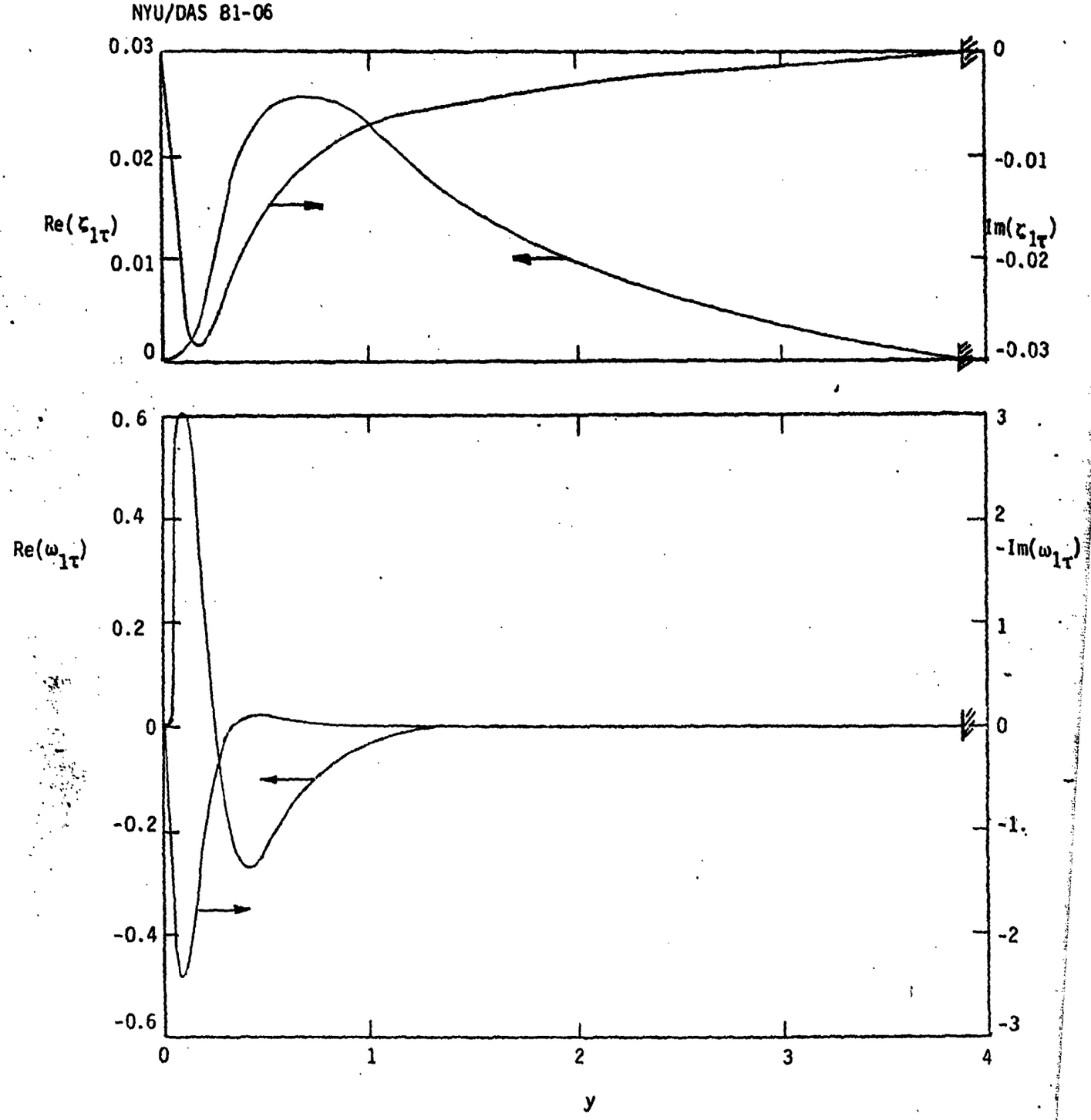

FIGURE 4: The τ - derivatives of the normalized perturbation stream function $\zeta_1(y,\tau)$ and the normalized perturbation vorticity $\omega_1(y,\tau) = (\zeta_{1yy} - \alpha^2\zeta_1)$ at time $\tau = 0$ according to the extended Meksyn and Stuart model.

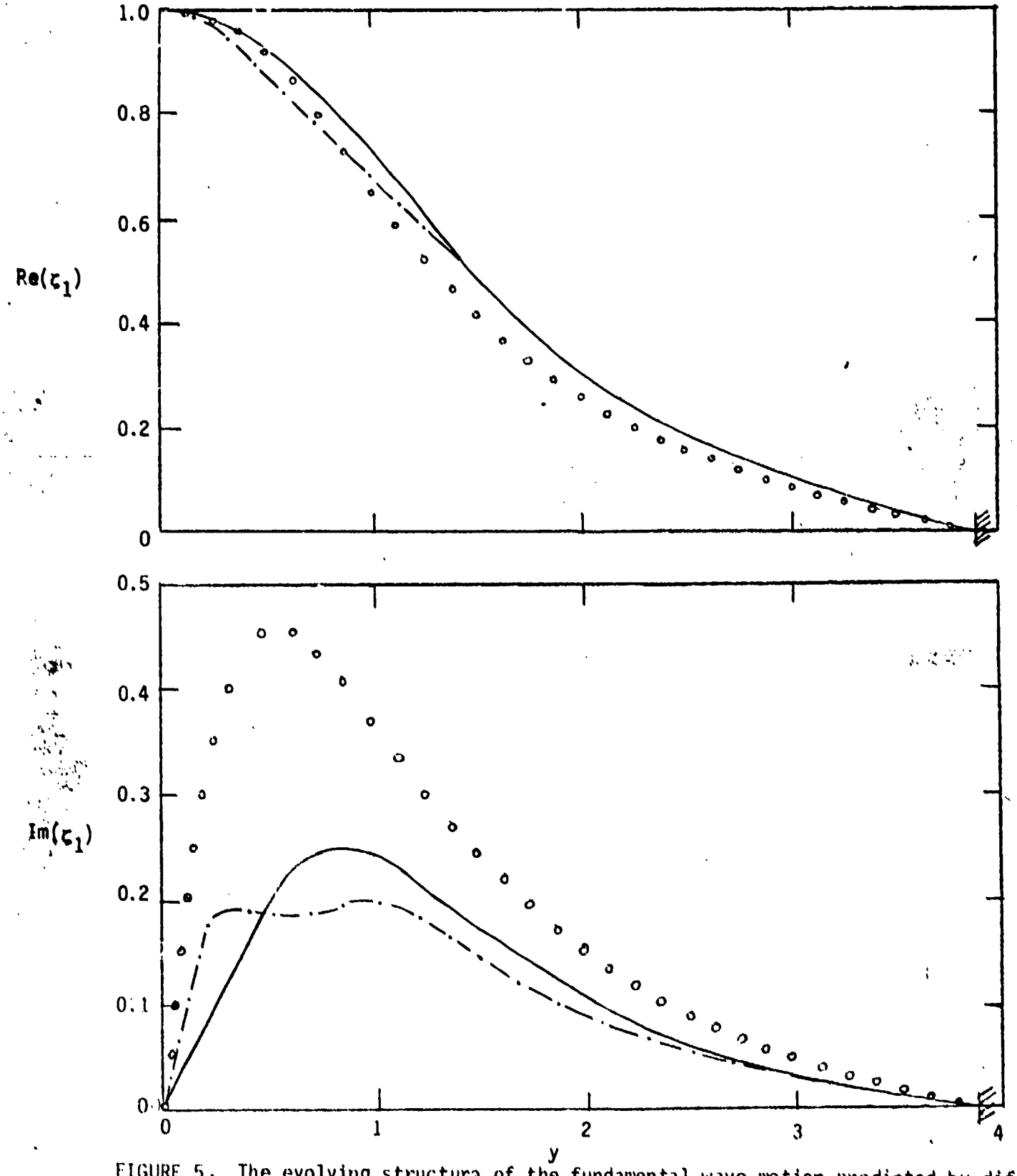

FIGURE 5. The evolving structure of the fundamental wave motion predicted by different models at selected times preceding saturation. o o o t = 0; — · — t = 9.82, extended Meksyn and Stuart model; ——— t = 9.82, nonlinear model. a) The normalized perturbation stream function $\zeta_1(y,t) = \phi_1(y,t)/\mathrm{Re}[\phi_1(0,t)]$

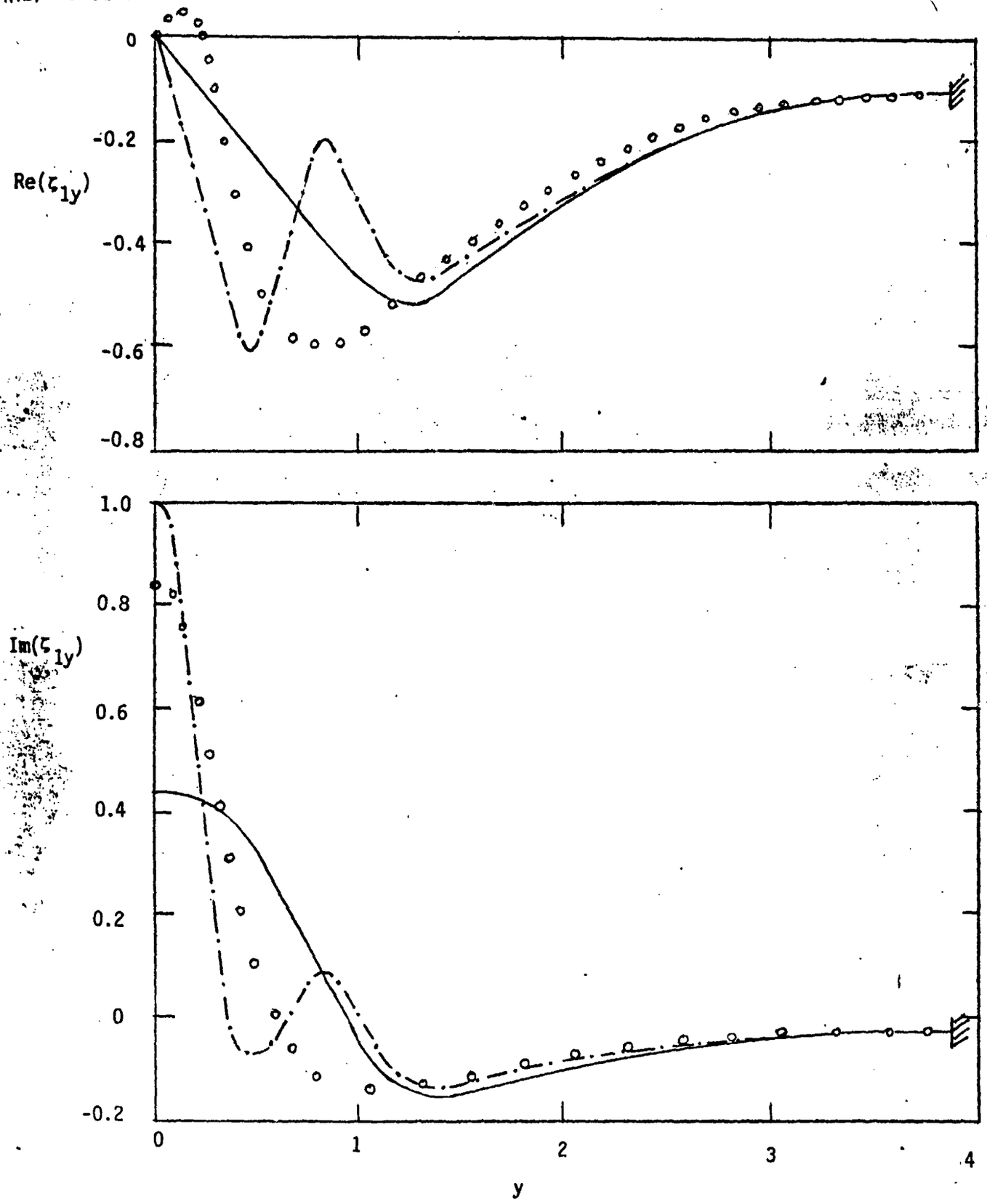

FIGURE 5: (Cont'd) b) The normalized streamwise perturbation velocity $\zeta_{1y}(y,t) = \phi_{1y}(y,t)/\mathrm{Re}[\phi_1(0,t)]$.

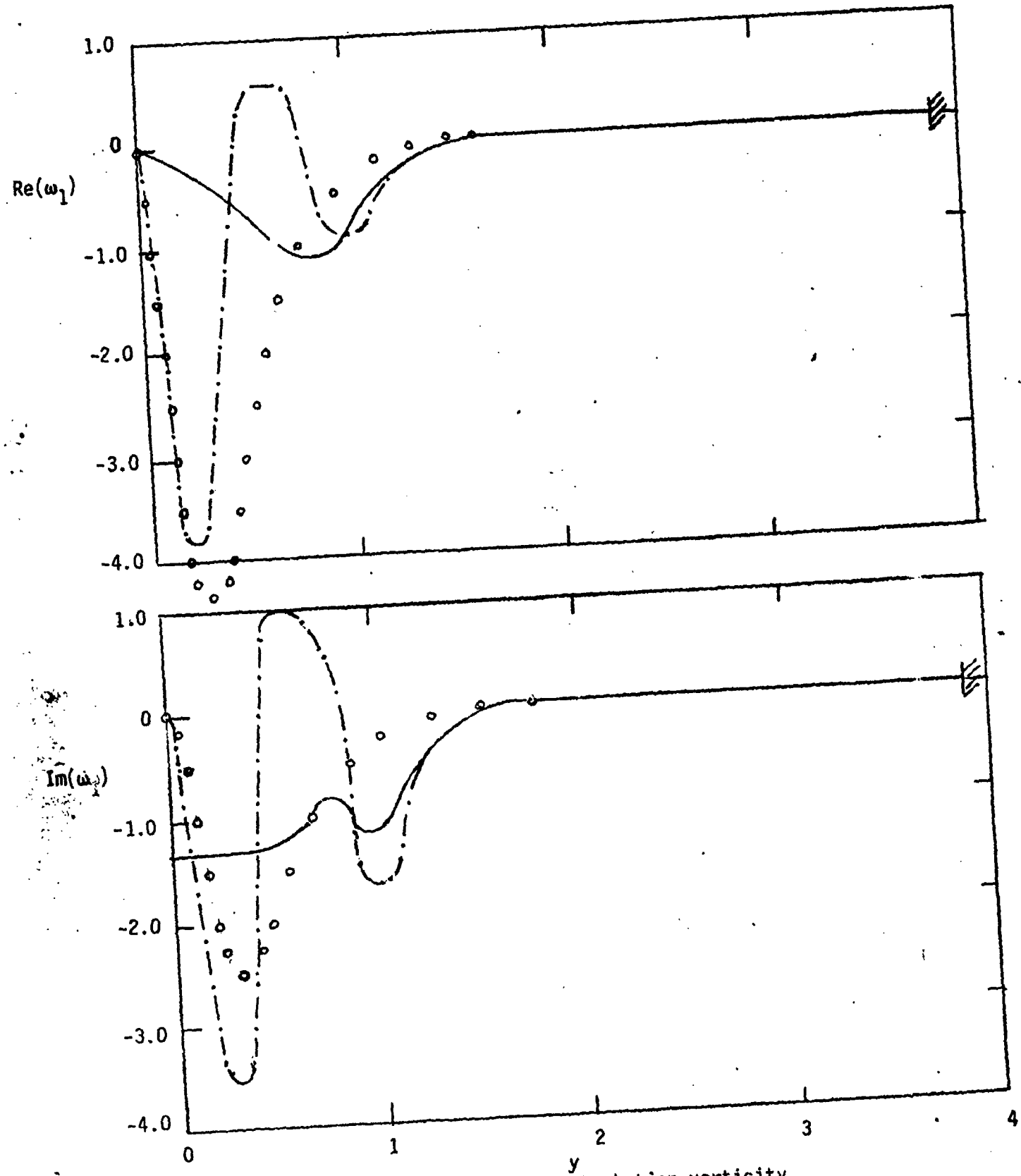

FIGURE 5 (Cont'd) c): The normalized perturbation vorticity $\omega_1(y,t) = [\phi_{1yy}(y,t) - \alpha^2\phi_1(y,t)]/\mathrm{Re}[\phi_1(0,t)]$.

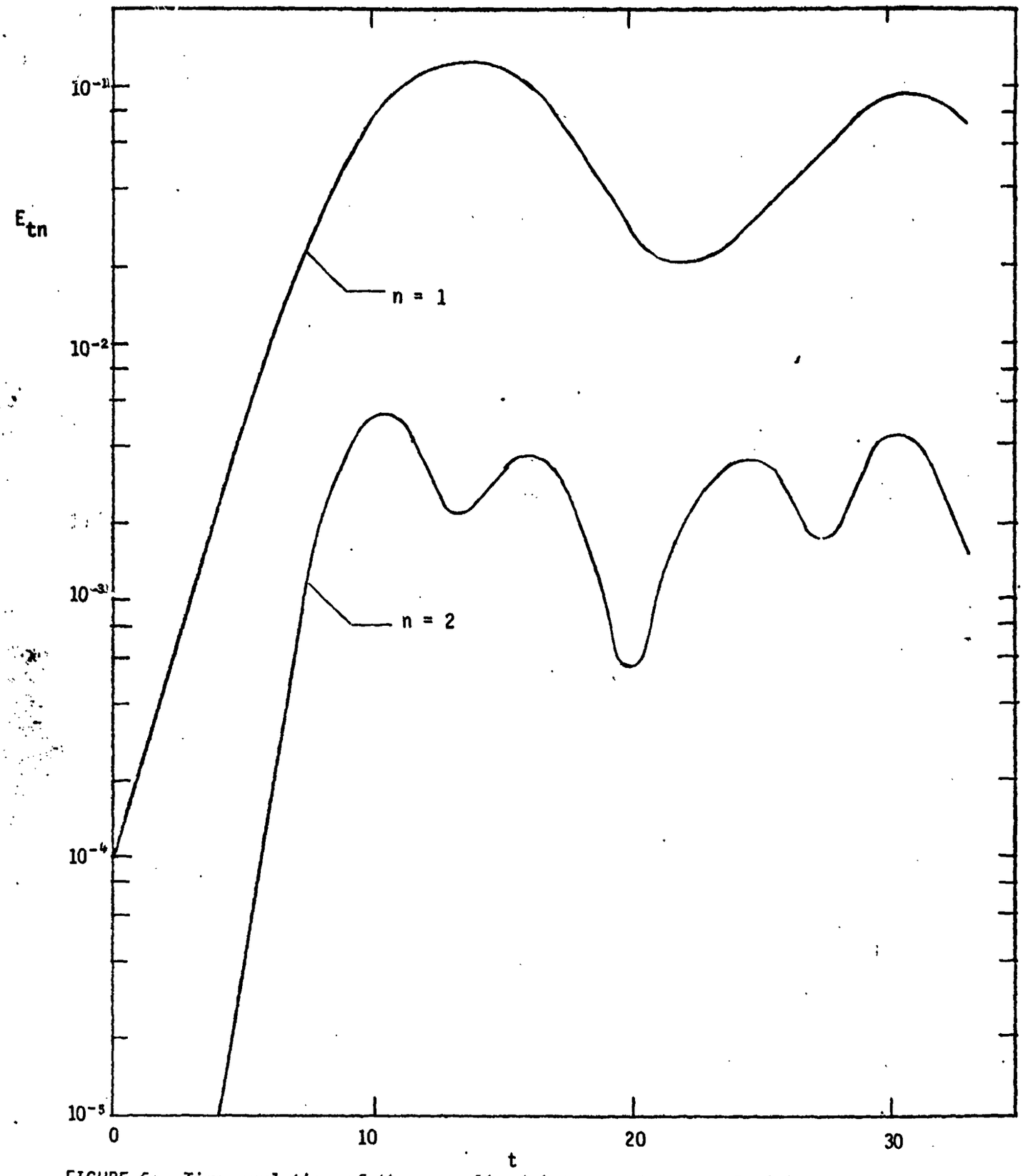

FIGURE 6: Time evolution of the normalized integrated energy $E_{tn}(t)$ of the fundamental (n=1) and the second harmonic (n=2) when subharmonics are suppressed. Nonlinear model.

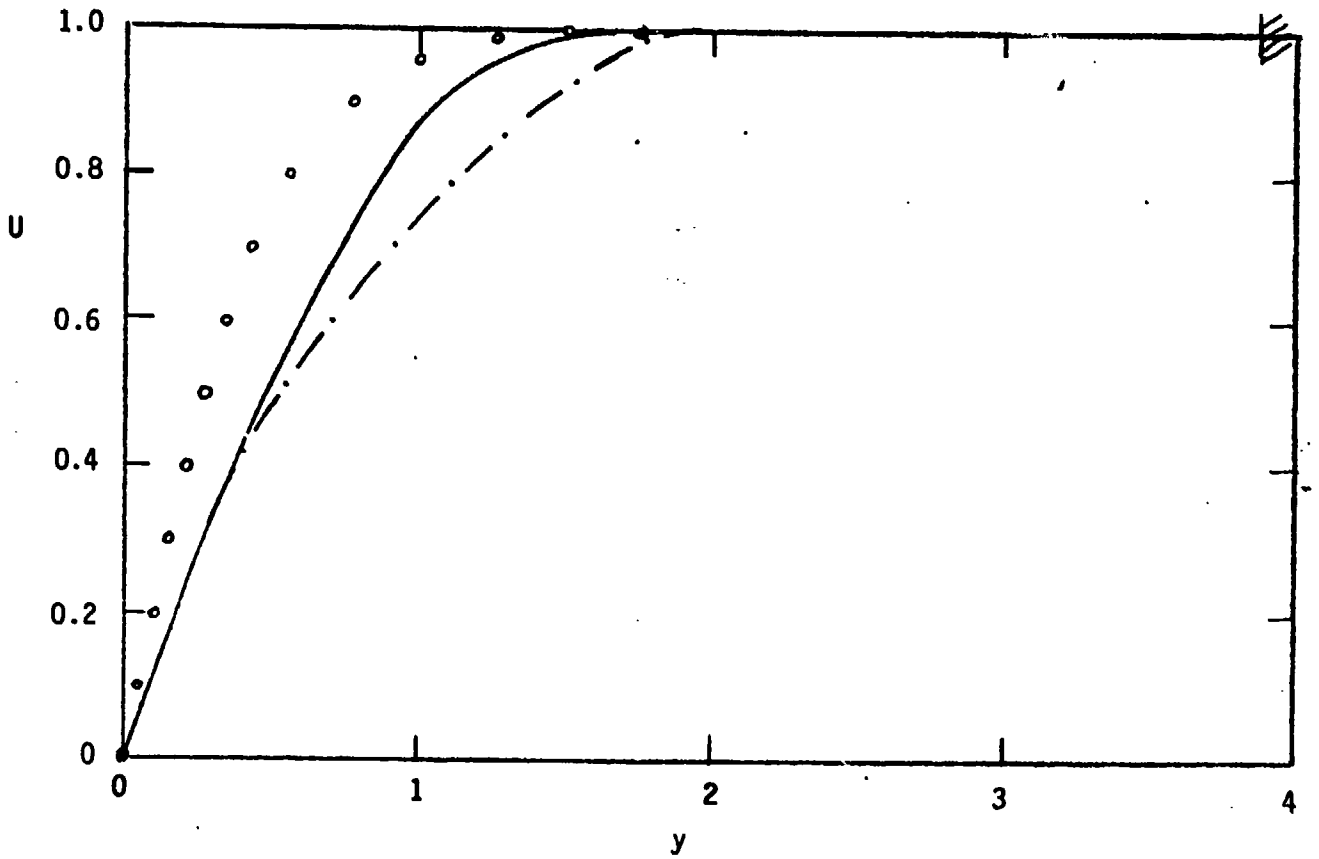

FIGURE 7: The evolution of the mean velocity profile U(y,t) at selected times preceding saturation of the fundamental. Nonlinear model. ooo, t = 0; ——, t = 9.82; —·—, t = 13.5.

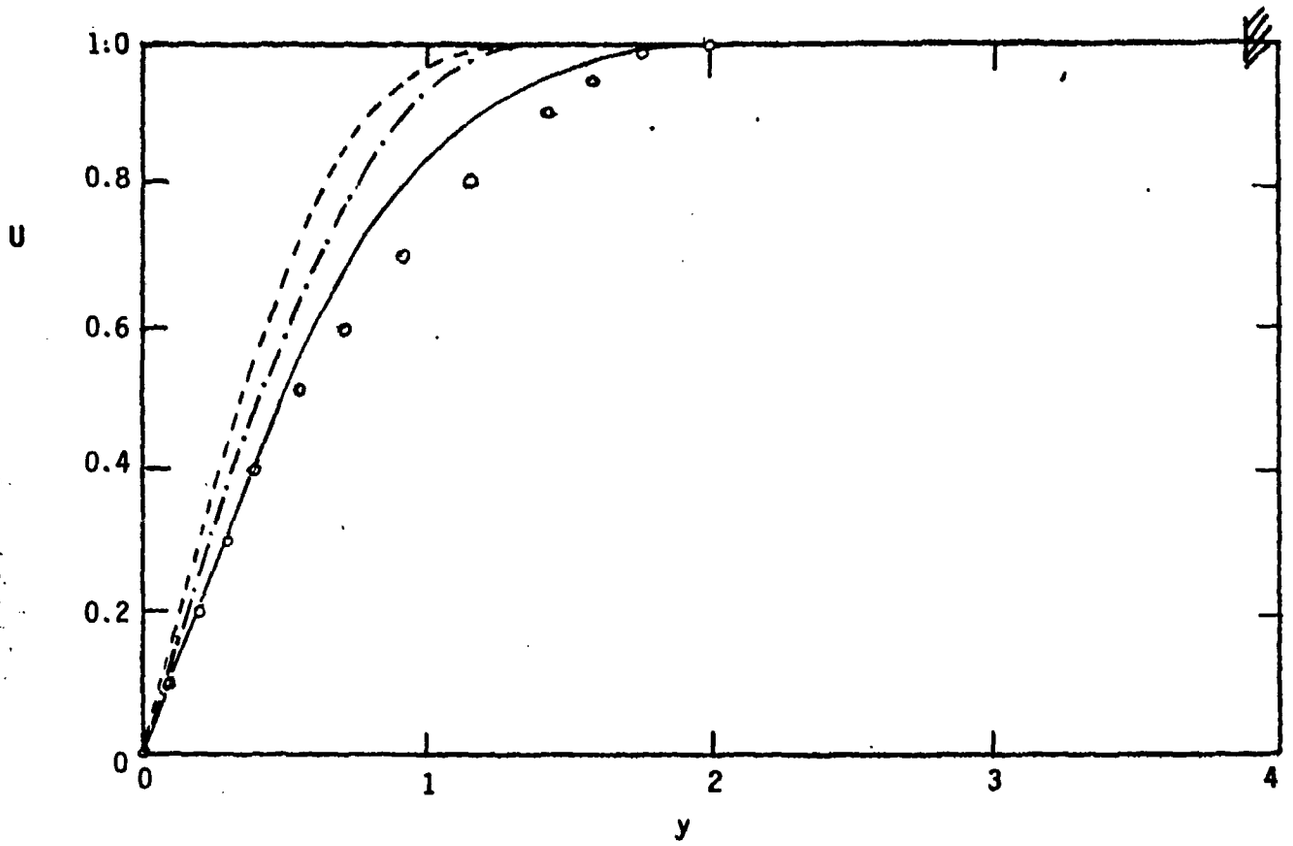

FIGURE 8: The evolution of the mean velocity profile U(y,t) at selected times following saturation of the fundamental. Nonlinear model with subharmonics suppressed. o o o, t = 13.5; —— . ——, t = 19.5 and t = 25.75; — — —, t = 22.15; ———, t = 30.55.

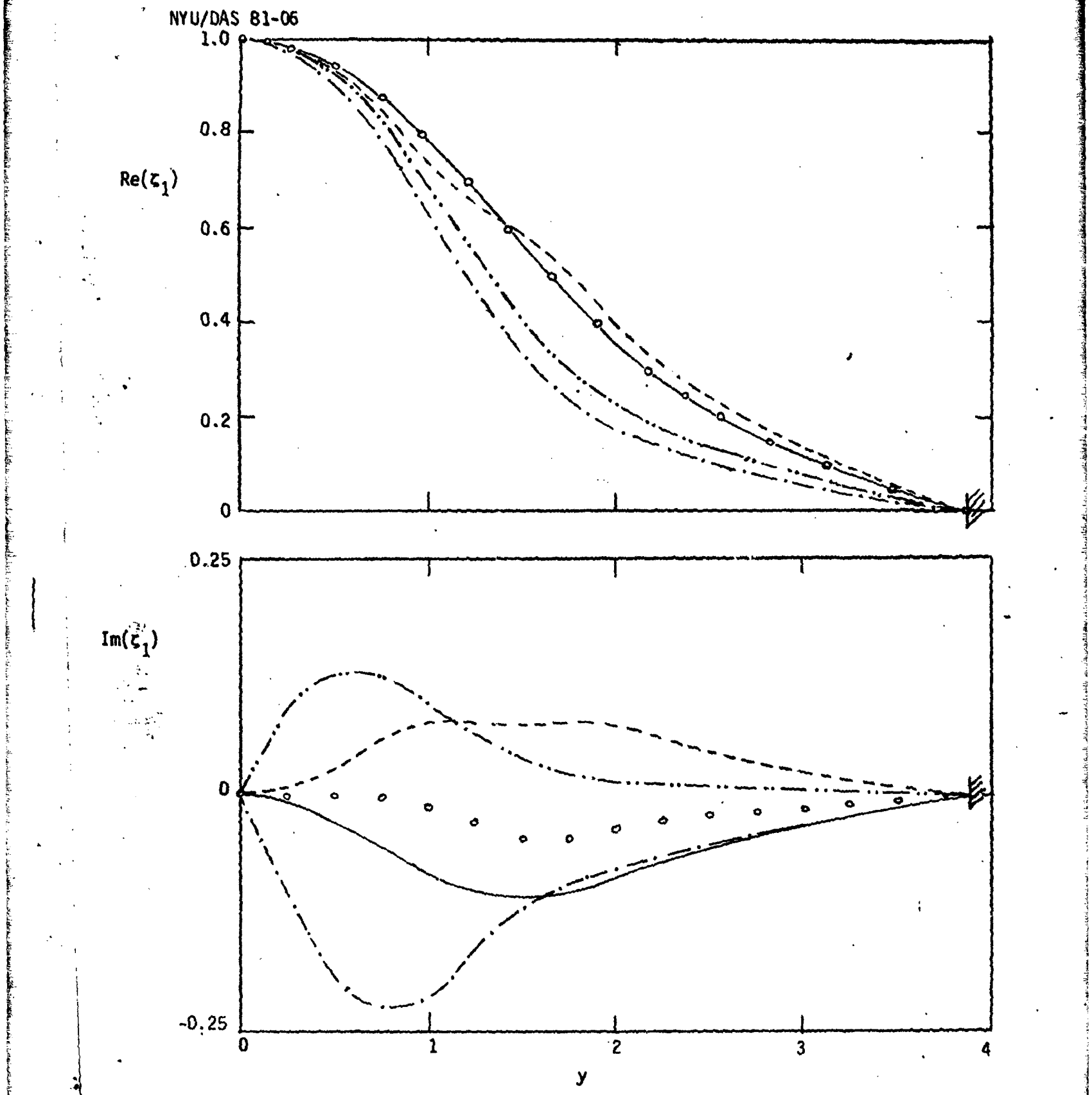

FIGURE 9: The evolving normalized stream function $\zeta_1(y,t)$ of the fundamental wave motion at selected times following its saturation. Nonlinear model with subharmonics suppressed. o o o, t = 13.5; ——·——, t = 19.15; — — —, t = 22.15; —··—, t = 25.75; ——— t = 30.55.

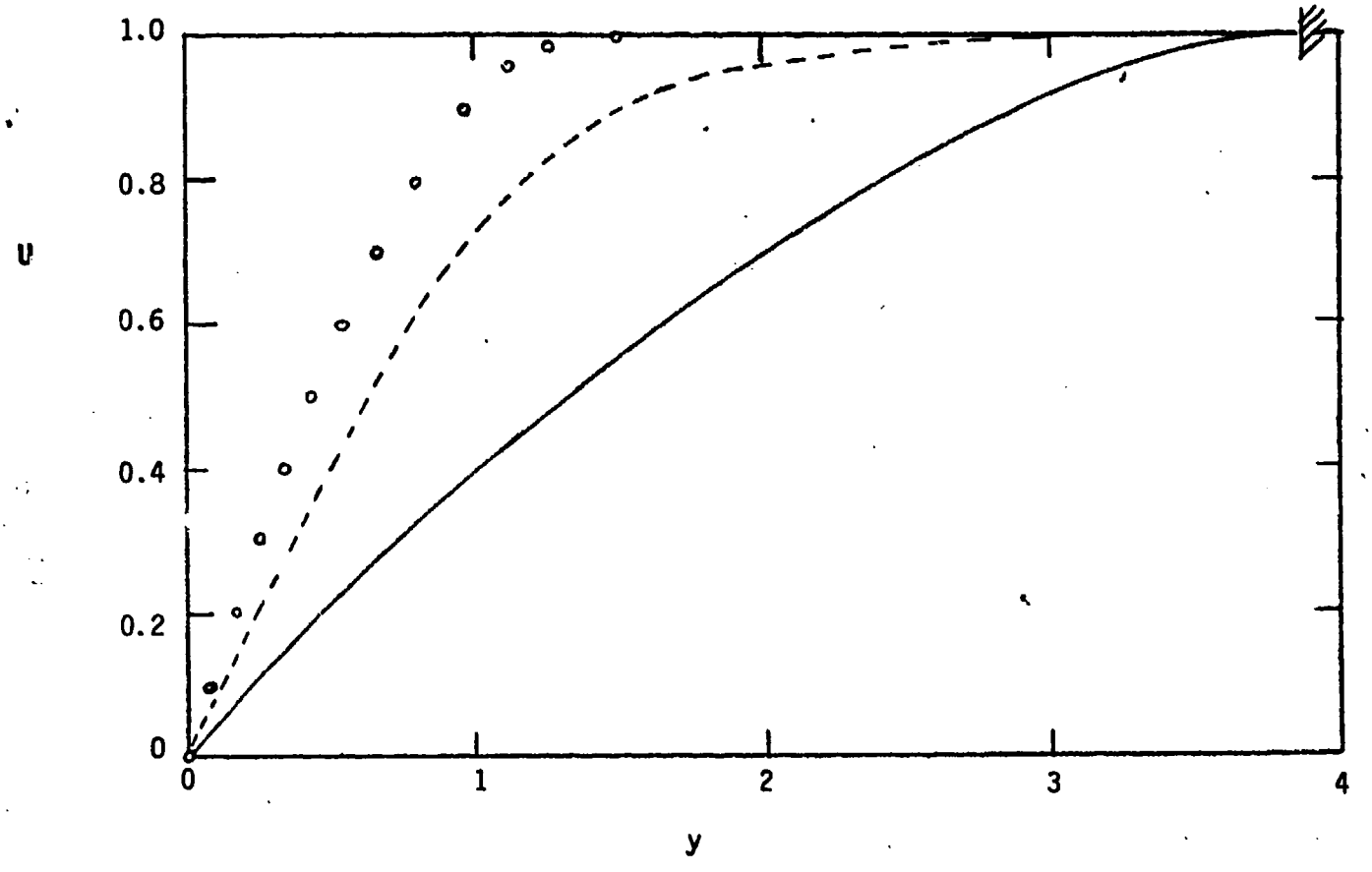

FIGURE 10: The evolution of the mean velocity profile U(y,t) at selected times following excitation of the 1/2 subharmonic. Nonlinear model. o o o, t = 17; — · — —, t = 22.4; ——— t = 30.2.

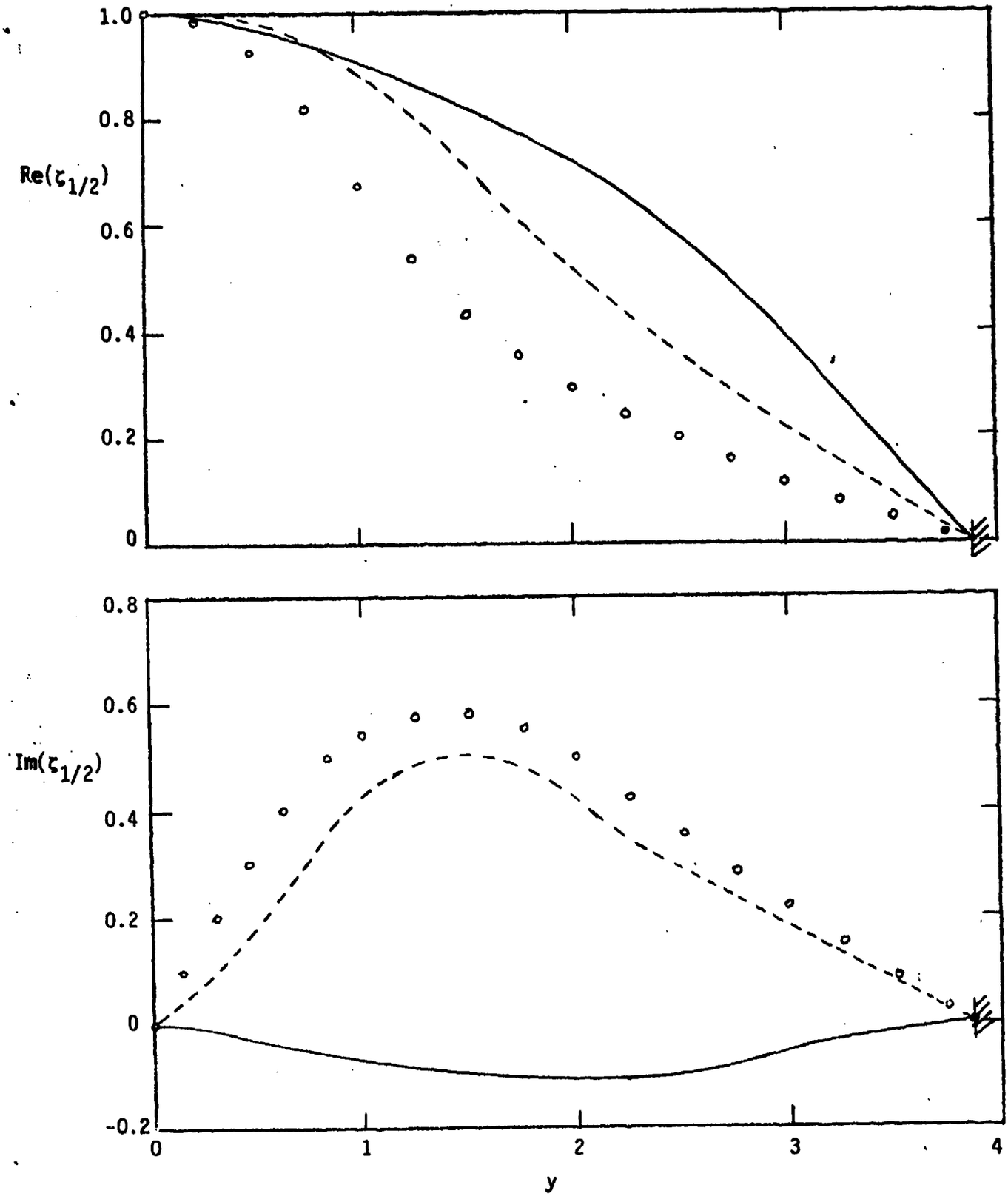

FIGURE 11: The evolving normalized stream function $\zeta_{1/2}(y,t)$ of the subharmonic wave motion at selected times following its excitation. Nonlinear model. o o o, t = 17; — — —, t = 22.4; ——— t = 30.2.

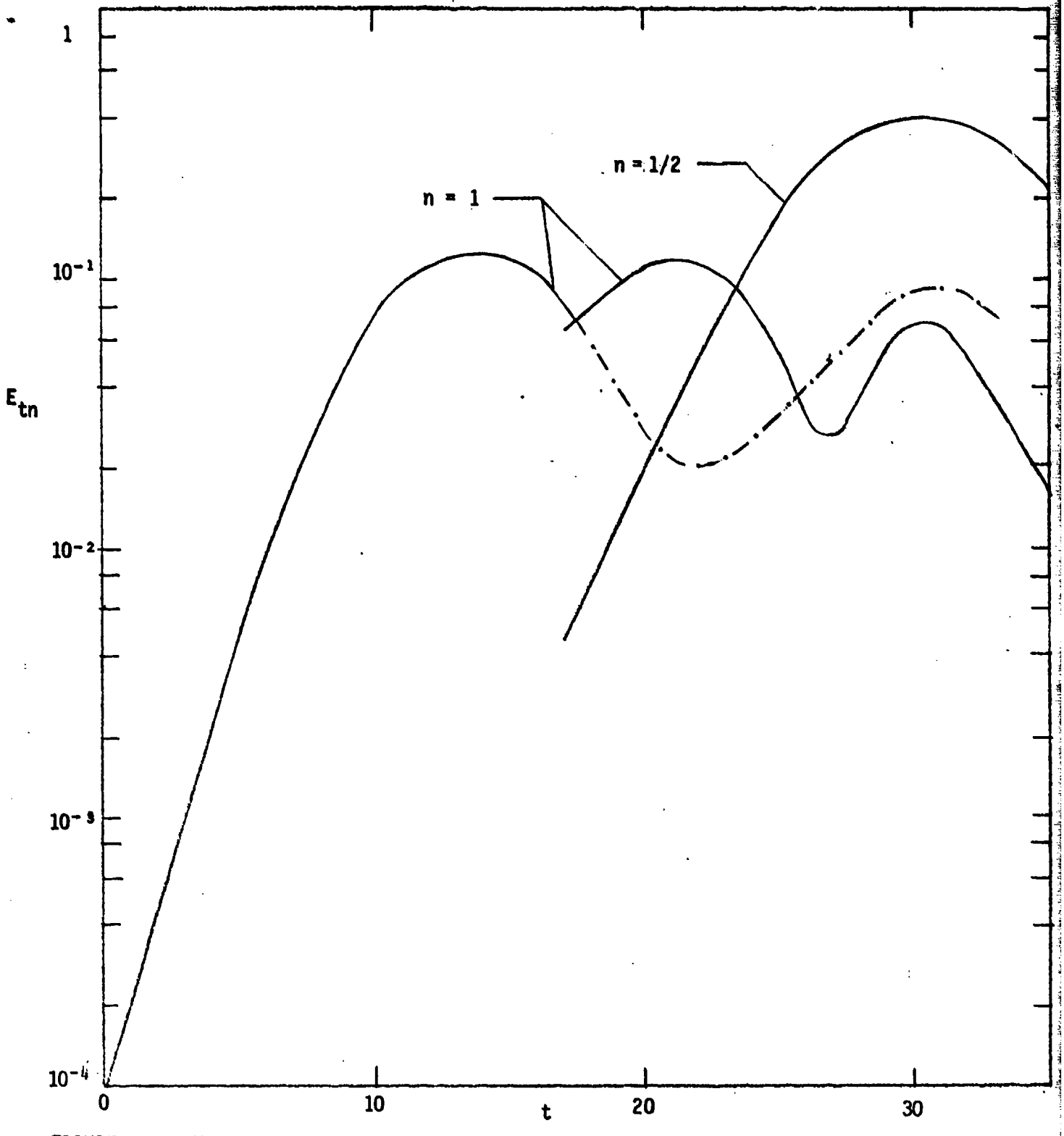

FIGURE 12: Time evolution of the normalized integrated energy $E_{tn}(t)$ of the fundamental (n = 1) and of the subharmonic (n = 1/2), the latter being excited at t = 17. Nonlinear model.